AFCRL-63-4

SATELLITE-TO-SATELLITE PROPAGATION EXPERIMENT FEASIBILITY STUDY AND PRELIMINARY DESIGN

John D. Meyer

Lockheed Missiles & Space Company
Sunnyvale, California

CONTRACT NO. AF19(628)-457
Project No. 4603
Task No. 460307

Scientific Report No. 1

11 Dec 1962

Prepared
for

ELECTRONICS RESEARCH DIRECTORATE
AIR FORCE CAMBRIDGE RESEARCH LABORATORIES
OFFICE OF AEROSPACE RESEARCH
UNITED STATES AIR FORCE
BEDFORD, MASSACHUSETTS

AFCRL-63-4

SATELLITE-TO-SATELLITE PROPAGATION EXPERIMENT FEASIBILITY STUDY AND PRELIMINARY DESIGN

John D. Meyer

Lockheed Missiles & Space Company
Sunnyvale, California

CONTRACT NO. AF19(628)-457
Project No. 4603
Task No. 460307

Scientific Report No. 1

11 Dec 1962

Prepared
for

ELECTRONICS RESEARCH DIRECTORATE
AIR FORCE CAMBRIDGE RESEARCH LABORATORIES
OFFICE OF AEROSPACE RESEARCH
UNITED STATES AIR FORCE
BEDFORD, MASSACHUSETTS

NOTICES

Requests for additional copies by Agencies of the Department of Defense, their contractors, and other Government agencies should be directed to the:

ARMED SERVICES TECHNICAL INFORMATION AGENCY
ARLINGTON HALL STATION
ARLINGTON 12, VIRGINIA

Department of Defense contractors must be established for ASTIA services or have their 'need-to-know' certified by the cognizant military agency of their project or contract. All other persons and organizations should apply to the:

U. S. DEPARTMENT OF COMMERCE
OFFICE OF TECHNICAL SERVICES
WASHINGTON 25, D. C.

ACKNOWLEDGEMENT

This study has been performed within the Research and Engineering Branch of Lockheed Missiles and Space Company, Sunnyvale, California, and represents the combined efforts of persons in a number of scientific disciplines. Contributions were made by Virgil A. Counter and Edward Eng in Ionospheric Propagation, by Arnold D. Daniel Jr. in capsule and ejection mechanism design, by Wayne Brewer in thermodynamic analysis, and by John B. Newman in orbital mechanics, and without their efforts the author could not have completed this study. The constructive suggestions and cheerful assistance of a large number of the author's colleagues are gratefully acknowledged.

ABSTRACT

The effects of the ionosphere upon radio frequency electromagnetic waves are discussed. Several types of satellite-to-satellite propagation experiments are presented, and the problems of implementation are delineated. The equipment around which the experiment must be designed is described, as are the vehicles available in Program 162. The relative merits of the various vehicles and the basis for the selection of the experimental configuration are discussed. The preliminary design results are shown.

CONTENTS

ILLUSTRATIONS

Section 1
INTRODUCTION

Operation of a satellite-to-satellite radio propagation experiment must be based upon a thorough knowledge of the experimental medium, the experimental environment, and the effects thereof upon the experiment. This report presents the results of a feasibility study and preliminary design effort directed at such an experiment.

It was anticipated that the experiment should include two transmitters, both in the frequency range from 3 Mc to 20 Mc, and would operate from a suitable vehicle, such as the Lockheed Agena. An ejected satellite was expected to transmit to the Agena-type vehicle. The experiment was anticipated to last approximately one week.

The feasibility study was to consider the frequencies to be used, the method of synchronizing the receivers with the transmitters (which were to operate alternately), the pulse length and repetition frequency, expected characteristics of the received signals, relative orbital positions of the transmitting and receiving vehicles, and problems attendant to conducting the experiment on a Program 162 vehicle. The preliminary design was to consider the ejection mechanism, the propulsion rocket (if used), the power supply, telemetry system, antennas, beacon transmitter, control unit, and an analysis of thermodynamic and other associated problems.

Section 2
FEASIBILITY STUDY

2.1 IONOSPHERIC PROPAGATION EFFECTS*

2.1.1 General

An electromagnetic wave propagating through the atmosphere is affected by many phenomena. The variation of the index of refraction in the troposphere (that portion of the atmosphere up to 65 km altitude) and in the ionosphere (that portion of the atmosphere above 65 km altitude) introduces phase shifts and refraction, causing apparent deviations in range, angular position, velocity (Doppler frequency), and attenuation (through ray path divergence).

In the troposphere, the wave is attenuated primarily through absorption by water droplets and ice formations. In the ionosphere, further attenuation is produced by absorption and scattering due to the appreciable number of free electrons from x-ray and ultraviolet radiation. Also, the frequency and polarization dependence of the index of refraction causes non-linear phase shift effects and polarization variations (Faraday effect), respectively. Non-linear phase shifts produce distortion (pulse dispersion) in the information content of the electromagnetic wave. Because the scope of the satellite-to-satellite experiment is concerned mainly with propagation within the ionosphere, the effects of absorption, refraction, Faraday rotation, pulse dispersion, and Doppler shifts will be discussed in the following subsections.

---

*The discussion in this section is primarily the work of Mr. Virgil A. Counter and will be included, in expanded form, in Space Age Electromagnetics – Volume II: Propagation, McGraw-Hill, to be published in 1963.

2.1.2 Attenuation

Molecular and ionic absorption and refractive attenuation are the primary causes of signal attenuation in the ionosphere. The absorption process involves a real transfer of energy from the wave via the electrons to the gas particles, while variations in refractive index result in an apparent attenuation of energy.

In the upper atmosphere, incident x- and ultraviolet radiation are absorbed somewhat selectively by the atmospheric constituents, resulting in a more or less stratified region of partially ionized gas, which is referred to as the ionosphere. The lowest region is the D-Layer at 85 km and the uppermost is the F_2 Layer at about 290 km. It is characteristic of the ionosphere that its electrical properties are a function of frequency. The highest frequency which is reflected by a given layer is termed the critical frequency ω_c for that layer. The critical frequency is related to the local plasma frequency ω_p, which is defined by

$$\omega_p = 56.3\sqrt{N} \qquad \text{(mks units)} \tag{2.1}$$

where N = local electron density.

The relation between ω_c and ω_p is given by

$$\omega_c = \omega_{pmax} = 56.3\sqrt{N_{max}} \tag{2.1a}$$

where the subscript max refers to the maximum for the layer in question. The reflection process is very similar to that found in metals. The ionospheric electrons are caused to move by the incident field, but their motion lags the electric field by 90 deg (in the lossless case), while the displacement current leads by 90 deg. When the two currents are equal in magnitude, reflection is complete. If, however, there are numerous neutral and ionized gas particles (as indeed there are in the ionosphere),

then a second process is involved. The electrons will now suffer a number of collisions each second and, with each collision, the electrons will lose part of its kinetic energy. Thus, while reflection will still occur, the process is no longer lossless so far as the electromagnetic field is concerned.

Refractive attenuation results from the divergence of the ray paths, which is caused by the variation of the index of refraction. The gross structure of the atmosphere contributes to that portion of the refractive attenuation which usually is positive and actually attenuates the signal. However, for situations in which the ionosphere is traversed by the signal, the refractive attenuation can be negative and the signal can be enhanced by the effect of refraction. Local inhomogeneities can cause this refractive attenuation to fluctuate positively and negatively at amplitudes of many db at VHF and lower frequencies. Therefore, at certain periods during the fluctuations, signal enhancement caused by refraction may more than offset the attenuation due to absorption and scattering.

As implied in the above discussion on absorption, the critical frequency and, therefore, the refractive ionospheric attenuation are approximately proportional to the inverse square of the frequency and generally are negligible above 1000 mc for the most severe ionospheric conditions. At a frequency of 100 Mc, attenuation due to absorption is less than 1 db, but refractive fluctuations may be greater than 10 db. As the radio frequency approaches the ionospheric critical frequency, both the absorptive and refractive space-to-ground attenuations may become tens of db.

It has been shown* that the attenuation constant, α, is given by

$$\alpha = \frac{\omega}{\sqrt{2}\,C}\sqrt{-\left(1-\frac{\omega_p^2}{\omega^2+\nu^2}\right)+\sqrt{\left(1-\frac{\omega_p^2}{\omega^2+\nu^2}\right)+\frac{\nu^2}{\omega^2}\left(\frac{\omega_p^2}{\omega^2+\nu^2}\right)^2}} \quad (2.2)$$

(nepers/m)

where ν is the electron collision frequency and C is the velocity of light.

*E. C. Jordan, Electromagnetic Waves and Radiating Systems, Prentice – Hall, Inc. p. 673.

Figure 2-1 presents this relationship in a normalized form with ν/ω_p versus ω/ω_p with α/ω_p as a parameter. As an example, consider the case where f = 16 Mc ($\omega = 10^8$), f_p = 4 Mc ($\omega = 2.5 \times 10^7$), $\nu = 1.5 \times 10^3$. For these conditions it is found that α/ω_p is roughly 6×10^{-14} and $\alpha = 1.5 \times 10^{-6}$ db/m, or 2.8×10^{-3} db/nm. The effect of reducing frequency is seen if f is changed to 8 Mc ($\omega = 5 \times 10^7$); this yields $\alpha = 10^{-5}$ db/m or 1.85×10^{-2} db/nm. For the low collision frequencies typical of the ionosphere (see Fig. 2-2), α rises quite abruptly as ω approaches ω_p from above.

2.1.3 Faraday Effect

The earth's magnetic field causes the electrons of the ionosphere to deviate from their normal oscillatory paths when excited by the electric field of an electromagnetic wave. Therefore, the polarization of the forward scattered field from each electron is shifted slightly from that of the incident field. This accumulative shift of polarization as the wave propagates through the ionosphere is called the Faraday effect.

One aspect of this effect is the longitudinal Faraday effect, or Faraday rotation, which is a rotation of the polarization ellipse of an arbitrarily polarized plane wave. The amount of rotation depends on the component of the magnetic field along the wave normal and varies approximately as the inverse square of the wave frequency. At frequencies below 200 Mc, the transverse Faraday effect also is significant, but only when the wave normal is close to being perpendicular to the direction of the magnetic field. This effect can change the eccentricity of the polarization ellipse, causing a linearly polarized wave to become circularly polarized (or vice versa), or causing a circularly polarized wave to alter its sense. The transverse effect is proportional to that component of the magnetic field perpendicular to the wave normal and varies approximately as the inverse cube of the frequency.

A common method of analysis of the Faraday effect is to consider the original wave as splitting into two magneto-ionic components designated as the ordinary and extraordinary waves. The two components propagate independently with different phase

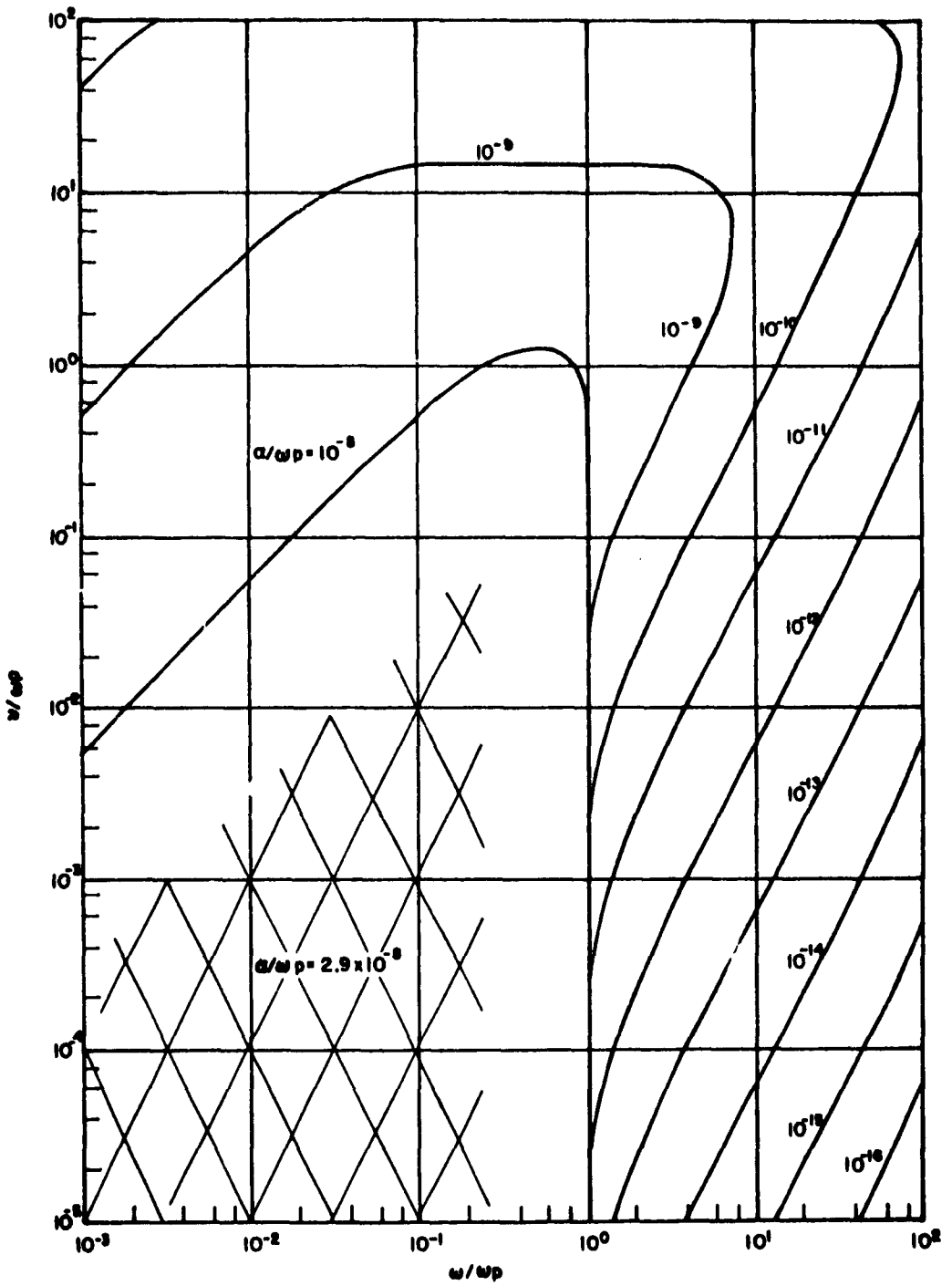

Fig. 2-1 Normalized Attenuation Constant

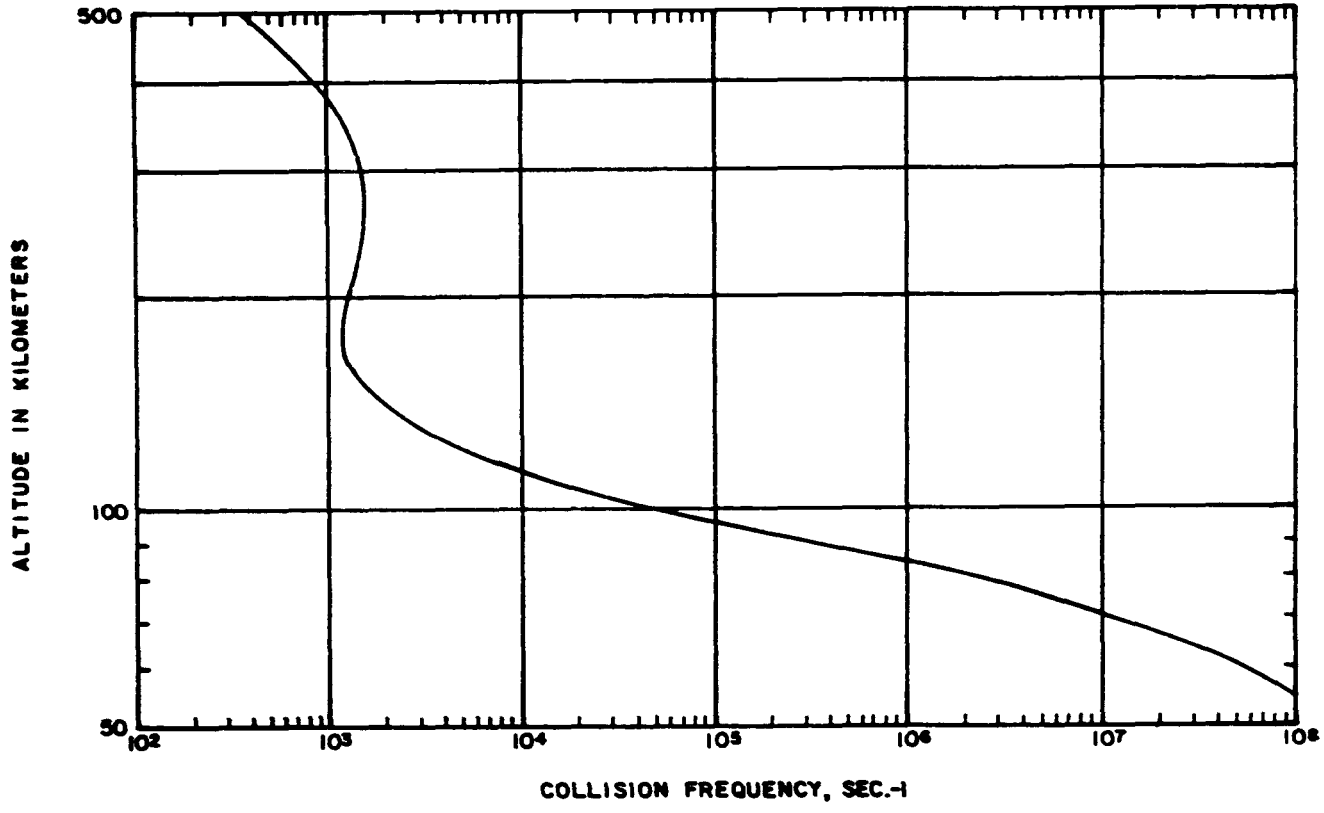

Fig. 2-2 Electron Collision Frequency Versus Altitude

velocities. The polarizations of the two components are orthogonal when absorption is not a problem. If the original signal is modulated and the delay difference between the two components is large compared to the periods of modulation, the Faraday effect would cause time-delay distortion of the received signal (unless only a single component is monitored). In pulsed transmissions, this distortion would increase the length or cause multiplicity of the pulses.

The magnitude of the Faraday effect may be calculated in terms of the relative phase shift between the two modes, given by

$$\Delta \varphi_F = \frac{\omega}{c} \int (\Delta n)\, ds \tag{2.3}$$

where $\Delta n = n_o - n_E$ = the difference in the indices of refraction for the two modes of propagation. This quantity may be written as

$$\Delta n = n_o - n_E$$

when n_o and n_E differ considerably, or, as

$$\Delta n = \frac{2\omega_p^2/\omega^2}{n_o + n_E} \left[\frac{\omega_H^4/\omega^4 \sin^4 \psi}{4\left(\frac{\omega^2 - \omega_p^2}{\omega^2}\right)^2} + \frac{\omega_H^2}{\omega} \cos^2 \psi \right]^{\frac{1}{2}} \left[1 - \frac{\left(\omega_H/\omega\right) \sin^2 \psi}{\frac{\omega^2 - \omega_p^2}{\omega^2}} - \frac{\omega_H^2}{\omega^2} \cos^2 \psi \right]^{-1} \tag{2.4}$$

when $n_o \approx n_E$ and where ω_M is the gyro frequency and ψ is the angle of the wave normal to the magnetic field. For the quasilongitudinal case, when n_o and n_E are very close to 1, and ψ is approximately zero

$$\Delta\varphi = \frac{1}{C} \left(\frac{\omega_p^2\, \omega_H}{\omega^2 - \omega_H^2} \right) ds \quad \text{rad/m} \tag{2.5}$$

and when ω_p and ω_H are constant

$$\Delta\varphi = \frac{1}{C} \frac{\omega_p^2 + \omega_H}{\omega^2 - \omega_H^2} R \tag{2.5a}$$

where R is the path length.

In the quasi-transverse case, when n_o and n_E are very close to 1, and ψ is approximately $\pi/2$

$$\Delta\varphi = \frac{1}{2\omega C} \int \left(\frac{\omega_p^2 \omega_H^2}{\omega^2 - \omega_p^2 - \omega_H^2} \right) \tag{2.6}$$

and when ω_p and ω_H are constant

$$\Delta\varphi = \frac{1}{2\omega C} \frac{\omega_p^2 \omega_H^2}{\omega^2 - \omega_p^2 - \omega_H^2} R \tag{2.6a}$$

Taking the case previously discussed (f = 16 Mc, f_p = 4 Mc) and using f_H = 1.3 Mc, (40 deg north latitude), the magnitude of the longitudinal effect is 1.7×10^{-3} rad/m (0.1 deg/m) and the magnitude of the transverse effect is 1.5×10^{-4} rad/m (0.009 deg/m) As ω approaches ω_p the magnitude of these effects increases rapidly.

The magnitude of the rotation of the polarization vector in the quasi-longitudinal case is one-half the phase shift between the two components. In the quasi-transverse case, however, the effect is rather complex and depends upon the polarization of the transmitted wave relative to the magnetic field of the earth.

2.1.4 Pulse Dispersion

If the phase delay through a medium increases linearly with frequency, the signal modulation is only shifted in time, with no distortion. Therefore, any medium which introduces non-linear phase delays will distort any modulation on a passing signal. This distortion may be estimated with the aid of an analysis by Elliott* and some reasonable generalizations. Elliott derived an equation for the shape of a single, originally rectangular pulse after it has traveled through a lossless section of waveguide. He assumed that the phase constant is proportional to the phase delay and can be represented by the first three terms of the Taylor series. With these conditions, Elliott's expression can apply to the distortion of a rectangular pulse in any dispersive homogeneous medium for which $\frac{\partial^2 \Phi}{\partial \omega^2} < 0$ and $\omega T >> 1$. His results were expressed as

$$\gamma = \frac{4}{T}\left(-\frac{1}{2}\frac{\partial^2 \Phi}{\partial \omega^2}\right)^{1/2} \simeq \frac{2}{fT}\left(\frac{Q}{\pi c f}\right)^{1/2} \qquad (2.7)$$

where

Φ = actual phase delay over the path of wave propagation

f = carrier frequency

ω = angular carrier frequency

T = time duration of the pulse

c = velocity of light in free space

Q = $80.6 \int N\, dR$ = a function proportional to the integrated electron density along the path of wave propagation

N = electrons per cubic meter

dR = meters

---

*R. S. Elliott, "Pulse Waveform Degradation due to Dispersion in Waveguide," IRE Transactions on Microwave Theory and Techniques, Vol. MTT-5, No. 4. Oct 1957, pp. 254-257.

Thus, for a given pulse width, frequency and Q, the amount of pulse distortion may be approximated by using the above equation. Figure 2-3 shows the pulse shape for several values of γ.

Elliott's results also may be applied qualitatively to a train of pulses. It is estimated from Fig. 2-3 that, for $\gamma = 1$, the effective signal-to-noise ratio for a pulse train would be reduced by approximately 3 db. In fact, the pulse degradation with this value of γ indicates the difficulty in the resolution of pulses with a time between pulses equal to the pulse widths. Therefore, it appears that the maximum distortion permissible for a high data rate pulse modulation is when $\gamma = 1$. In the case of an inhomogeneous and turbulent ionosphere, this value may be much less.

Considering the specific case where f = 16 Mc, T = 250 μs, prf = 10, and the electron density is constant at $2 \times 10^{11}/M^3$ (f_p = 4 Mc), it is found that $\gamma = 1.27 \times 10^{-5}$ Therefore, the criterion cited above, $\gamma = 1$, will be obtained when the separation reache 79 km (42.5 nm) and it must be expected that at the peak of the F_2 region, pulse shape degradation will cause a serious drop in the instantaneous peak power received.

2.1.5 Doppler Effect

The relative radial velocity component of a transmitting or receiving source can be determined from the frequency difference (or Doppler frequency) shift between the two signals. In free space, this Doppler frequency can be expressed as

$$f_r - f = f_{D_{fs}} = -\frac{f}{c} \dot{R} \qquad (2.8)$$

where

fr = received frequency

$f_{D_{fs}}$ = Doppler frequency in free space

$\dot{R}$ = relative radial velocity between the transmitter and receiver

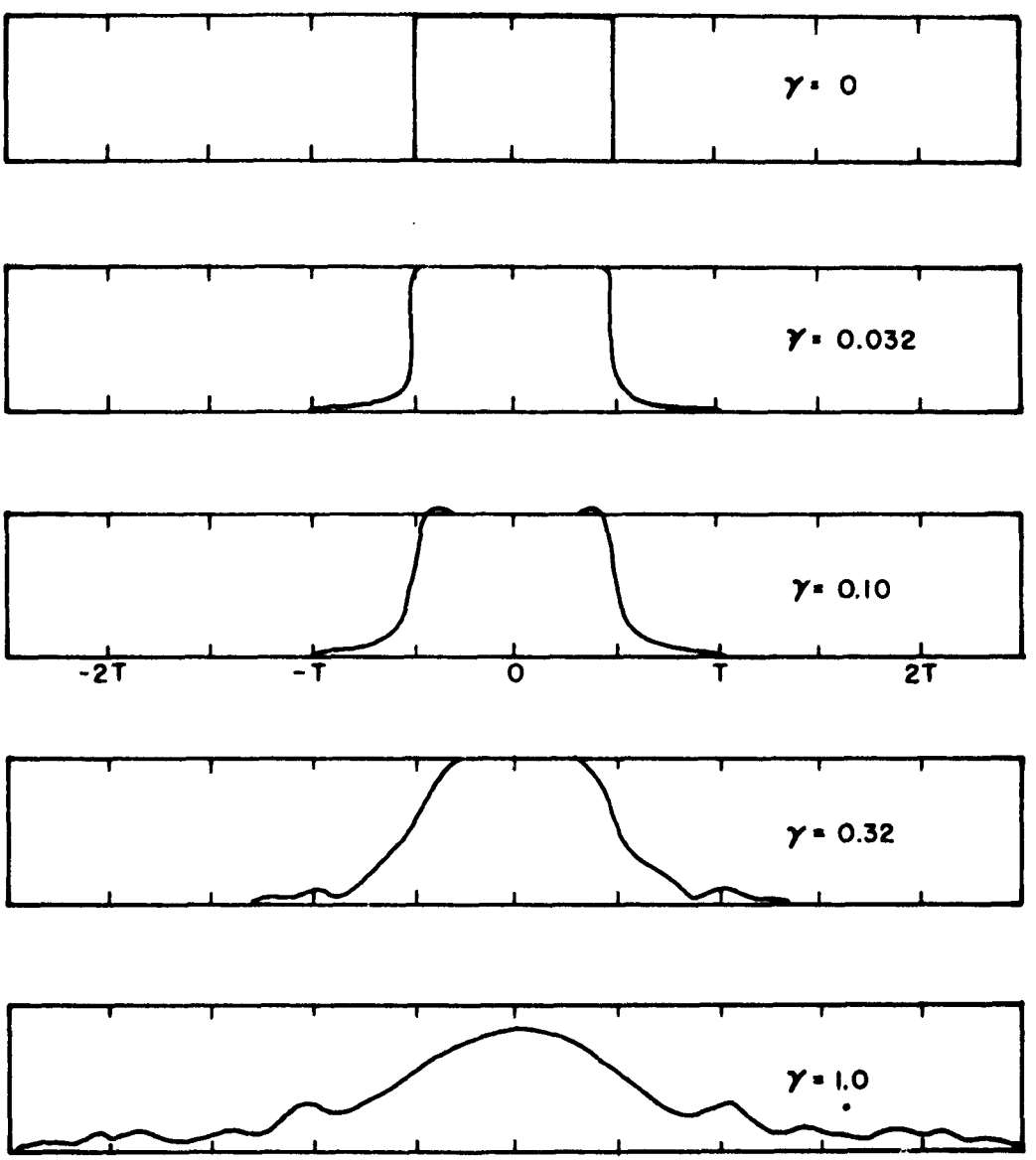

Fig. 2-3 Pulse Distortion in a Dispersive Medium (After Elliott)

During actual measurements, this equation would represent the average one-way frequency difference over a finite time interval.

For the dispersive ionosphere, the apparent relative radial velocity will be a function of frequency and the Doppler equation must be written

$$f_{D_m} = -\frac{f}{c}\frac{d}{dt}\int\left(1 - \frac{80.62\,N}{f^2}\right)^{1/2} ds = \frac{f}{c}\frac{d}{dt}\int\left(1 - \frac{f_p^2}{f^2}\right)^{1/2} ds \qquad (2.9)$$

if the collision frequency is small relative to f. Use of two or more frequencies, coherent with one another, will permit measurement of the Doppler component resulting from the dispersive nature of the medium, and thus will yield the integrated electron density between the transmitters and the receivers. In the case where N is constant along the path, the Doppler frequency becomes

$$f_{D_m} = -\frac{f}{c}\, n\, \dot{R} \qquad (2.9a)$$

where it must be remembered that n contains a factor of $\frac{1}{f^2}$ and then the frequency dependence and range change rate dependence are obvious.

An idea of the magnitude of the dispersive Doppler effect for slowly separating satellites can be obtained from the following calculation. Assume that $f_1 = 16$ Mc, $f_2 = 8$ Mc, $f_p = 4$ Mc, and $\dot{R} = 8$ m/sec.

$$f_{D_{fs}} = -4.3 \text{ cps at 16 Mc}, \; -2.15 \text{ cps at 8 Mc}$$

$$f_{F_m} = -4.15 \text{ cps at 16 Mc}, \; -1.86 \text{ cps at 8 Mc}$$

The Doppler components due to the medium are + 0.15 cps at 16 Mc and + 0.29 cps at 8 Mc – certainly not very large changes.

Thus, while the dispersive Doppler technique has been highly successful for ground to rocket measurements of integrated electron density, it is not a very good tool for measuring integrated electron density between two slowly separating satellites. This is not to imply that satellite-to-ground measurements are not feasible; these measurements can be performed much as in the case of the vertical rocket. The data reduction problem is more complex, however, because the data received relates to a number of ray paths, not just one. Furthermore, when the transmitting frequencies are close to local plasma frequency, the ray paths will be sufficiently different to degrade the data quite seriously.

2.2 EXPERIMENTAL APPROACHES

2.2.1 Sounding Approach

Previous radio frequency studies of the ionosphere have, of necessity, been confined either to a ground-to-ground, or a space-to-ground propagation mode of operation. Despite the limitations imposed by these restrictions, a number of effective experimental techniques have been developed and a wealth of data has been accumulated. A large fraction of the experimental ionospheric data has been acquired from vertical- or oblique-incidence, swept-frequency pulse soundings. Such techniques are equally applicable for "top sounding" from a satellite (or satellites) and can prove of great value in describing the upper reaches of the ionosphere.

2.2.2 Phenomenological Approach

A greater degree of freedom is afforded by transmission from satellite to satellite; this makes possible an entirely new type of operation, wherein both the transmitter and the receiver are located within the ionosphere. Under these conditions, it is

possible to study the ionospheric propagation effects mentioned in Section 2.1 above. The experiment can yield more useful data if the satellites are placed in an orbit such that the vehicles rise and fall in unison through the ionosphere. Because of the general incompatability of the top-sounder and the propagation effect approaches, they will, in this study, be considered separately; and though regions of overlap may exist, they generally will be ignored in this report.

2.3 EXPERIMENTAL TECHNIQUES

2.3.1 Experimental Geometries

A wide variety of techniques may be used to implement the two general approaches discussed above; for the sake of clarity, description of these techniques will also be kept quite general in the following.

A top-sounder experiment may be designed as a one-satellite operation, but, in the case where the experiment is of secondary importance to the satellite flight, it may prove necessary to separate the transmitter from the receiving satellite to avoid interference with primary payload operation. Such a two-vehicle experiment becomes, of necessity, an oblique-incidence sounder. A sounding experiment should be conducted from vehicles well above the peak of the ionosphere; thus an altitude of at least 500 to 1,000 nm is indicated.

A two-satellite ionospheric phenomena experiment may take several forms, depending upon the phenomena to be studied. Similar to the top sounder, but at ionospheric altitudes, an experiment could consist of two satellites relatively close together. Such a system could obtain data on Faraday rotation, multipath effects, pulse dispersion, attenuation, and, to a minor degree, ducting. In contrast, use of antipodal satellites would emphasize study of long range ducting effects and could obtain little or no data on other propagation phenomena.

Between these extremes any number of orbital geometries can be devised, each with its relative merits. Worth consideration is the set of geometries in which the vehicles vary in separation from minimum to maximum and vice versa a number of times during the life of the experiment. The number of times, of course, may be adjusted as desired.

2.3.2 Vehicular Considerations

Not only must a variety of geometries be considered in the experimental design, but the various ways in which these geometries can be achieved must be studied. This discussion, also, will be of a general nature and will not deal with specific vehicles. It is technically quite difficult to conduct an oblique-incidence top-sounding experiment between two satellites which are not placed in orbit by the same vehicle. However, if the satellite orbits do derive from the same launch, then vehicle separation can be achieved only by means of a continuous change in separation as the experiment progresses. Use of two launch vehicles to achieve a more or less fixed separation between satellites may be considered; but such a feat is roughly as difficult as achieving a rendezvous and requires precise synchronization on the ground and some degree of station-keeping capability in one of the satellites. It should be noted that a pure antipodal experiment requires almost as precise ground synchronization as the stabilized oblique sounder.

As mentioned previously, the experiment may be designed with a variable geometry; and this mode of operation can be obtained in several ways. The two satellite orbits may derive from a single launch and their initial separation rates may be increased from several feet per second to several hundred feet per second. Thus the time required to achieve vehicle opposition would range from several months to several days, depending upon altitude, with the lowest velocities providing a quasi-stationary state of operation.

The separate-launch, variable-geometry approach, where little if any attempt is made to control orbital parameters, will in general provide for an infinity of geometries. This approach also admits of multiple vehicle operation, including the special case wherein one vehicle has a sufficiently long operating life to operate with a number of short-lived vehicles launched sequentially. Such a possibility will be discussed at greater length in Section 3.3.2.

2.4 CONCLUSIONS

It has been shown that the propagation of high-frequency signals from one satellite to another will be affected in several ways. These effects are of sufficient magnitude as to be observable even when using relatively simple equipment on the satellites. Not only may ionospheric propagation phenomena be observed when transmitting from satellite to satellite, but it is also possible to operate a two-satellite ionospheric top sounder.

It should be understood that no experimental geometry permits studying all aspects of the ionosphere at one time. With some variable geometries, however, most ionospheric phenomena can be studied at one time or another during the lifetimes of the vehicles. Although almost any experimental geometry desired may be obtained, some are much easier to achieve than others and this may prove to be a controlling factor in the design of the experiment. Thus, it may be concluded that any one of a number of ionospheric propagation experiments are feasible; but prior to the selection of the experiment to be undertaken, it is necessary to weigh with great care the relative merits of both the possible experiments and the methods available for implementation of the experiments. The actual selection was part of the preliminary design phase and is discussed in the following section.

Section 3
PRELIMINARY DESIGN

3.1 GENERAL

The preliminary design of the satellite-to-satellite radio propagation experiment will be controlled by certain initial constraints. It was predetermined that two frequencies in the 3 to 20 Mc region should be used. The experiment will use a suitable vehicle to launch the second vehicle into an orbit approximately in the same plane as the mother vehicle, with the transmitter in the ejected package. It is anticipated that the mother vehicle will be an Agena and that the experimental lifetime will be about one week. As part of the second item of work (design and construction of an operating model) it is specified that the Government should furnish the transmitters, receivers, power converters, and antenna tuning units; these items, designed and built by General Electric Company, further define the experimental design. Several possible launching schemes will be investigated because the original concept appears to be too restrictive. Other than this one deviation, the preliminary design will proceed roughly as originally planned.

3.2 GOVERNMENT-FURNISHED EQUIPMENT

The Government-furnished General Electric transmitting and receiving units are solid-state, high-efficiency units designed to meet the temperature, vibration, and shock environments encountered in missile and satellite flights. The system consists of a transmitter programmer, two transmitters, two receivers, and an IF amplifier. The transmitters are frequency-controlled by a crystal and have a peak power output of 250 w up to 10 Mc (150 w, from 10 to 20 Mc). The nominal pulse width is 250 μsec, the prf is 10, and the average peak-power requirement of the transmitter is 1.9 w. The transmitter programmer unit consists of stabilized digital count-down circuits, which generate the correct prf and pulse width, and timing circuits, which select the correct transmitter.

Its power requirement is 0.72 w. The receivers are single-conversion superheterodyne units with the gain and noise figure commensurate with the received noise level. The power requirement of the receiver is 0.17 w, and the output frequency is 3 Mc. The IF amplifier has a 10-kc bandwidth centered at 3 Mc, a minimum gain of 72 db, an age range of 50 db, and age and video outputs. The power requirement of the IF strip is 0.44 w. All units require a 28-v power source except the programmer, which requires -12 v and +16 v, and the transmitter, which requires +16 v, +28 v, and +50 v. The "non-standard" voltages will be obtained from a 28-v power converter; however, this unit will not be GFE as required by the original contract.

It is anticipated that both receiver and transmitter specifications will be changed somewhat prior to delivery of these items, but the above represents presently available data furnished and confirmed by the manufacturer.

3.3 EXPERIMENTAL CONFIGURATIONS OBTAINABLE

Because of the dependence of experimental geometry upon specific launch vehicle details, the preliminary design effort was predicated upon the use of the basic Agena vehicle, as used in the LMSC Program 162. It is, therefore, essential that operations of this program be studied. It is the practice of the Air Force to utilize excess space and weight allowance on Program 162 vehicles for research payloads. These secondary payloads are placed in the Agena vehicle and carried into orbit on a non-interference basis. Research payload data are generally fed via two sixty-point-per-second commutators to a two-channel tape recorder. Upon ground command, the tape-recorded data is played back at high speed through the telemetry link. It is possible, following completion of the primary mission, to continue operation of the research payload with the primary vehicle functions shut down. By this means the experiment may be prolonged for a period of a week or so. Such a vehicle is frequently referred to as a "zombie." A further aspect of Program 162 is the planned installation of a large, self-propelled satellite on the Agena. This satellite, referred to as the P-11, is to be ejected once the Agena is in orbit, and it will then propel itself into one of two higher orbits. The typical Program 162 Agena has a perigee of 115 nm and an apogee between 225 nm and 380 nm and the P-11 will be in either a 200 nm circular orbit or in an orbit with a perigee of 115 nm and an apogee of 2,500 nm.

On the basis of these operations it is possible to define three basic modes of operation for a satellite-to-satellite experiment: (1) two Agenas, (2) an Agena and a P-11, or (3) an Agena and an ejected package. (The possibility of ejecting a package of the size envisioned here from a P-11 must be rejected because the general construction of the P-11 precludes such an operation.)

3.3.1 Concept 1

This concept, using two Agena "zombies," involves a rather complex and unpredictable geometry. Vehicles in Program 162 are placed into slightly elliptical orbits and the apogee is intended to be about 225 nm but occasionally it has been as high as 380 nm. This variation in apogee is random in nature, as is a variation in orbital period. The time of vehicle launch also is subject to large variations due to unforeseen problems encountered during launch operations. For these two reasons, it is not possible to predict in advance the inter-satellite geometry to be expected during the course of the experiment. It must be expected, for this concept, that during the experimental period the separation would be as great as one-half the earth's circumference and might be as small as a few hundred miles and probably would vary within these limits several times during the life of the vehicles

Given this experimental geometry, it is necessary that the experiment function at separations of up to 11,000 nm. Postulating the experimental study objective to be ionospheric ducting, multi-path communications and interference, antipodal effects, etc., it appears advisable to set one frequency several times greater than the maximum anticipated critical frequency of the F_2 region of the ionosphere to preclude incurring excessive signal loss. To study the same effects at times of significantly reduced ionospheric activity, the second frequency should be at least half the first frequency and yet should still be above the critical frequency of the F_2 region most of the time. To this end, it is suggested that the frequencies be roughly 7 Mc and 14 Mc. The transmitting package would consist of a pair of antennas, an antenna tuning unit, two transmitters, a programmer, a power converter, interconnecting wires, a container, and a control system which will activate the antenna erection

mechanism and the programmer. The transmitters would be keyed by the transmitter programmer and would transmit 250-μsec pulses with a peak power of about 150 w and a prf of 10. Each transmitter would operate for roughly 1/2 sec followed by 1/2 sec of no transmission, after which the other transmitter would be keyed. The keying could be coded for frequency identification. The power converter would be used to convert vehicle 28 vdc to the dc voltages required for the transmitters and the programmer. Total power consumption for the transmitting package would be 2.6 w.

The receiving package would consist of a pair of antennas, two receivers, an IF amplifier, interconnecting wires, a container, and a control mechanism which would turn on power to the receivers and the IF amplifier. Both receivers feed the IF amplifier simultaneously; therefore, it would be necessary to turn off the receiver not receiving the desired signal. The General Electric receivers would require a programmer to accomplish this. All receiving units require 28 vdc, and the power consumption of the package will be 0.75 w. The receiver-IF amplifier outputs are video, AGC, and peak envelope, and it would be planned to telemeter video to the Air Force ground tracking sites on a real-time basis during the command telemetry period and to record AGC and peak envelope for command dump.

Total weight for the transmitter is about 20 lb and for the receiver about 15 lb. Inasmuch as both vehicles would be tracked by Air Force telemetry stations, all information necessary to determine the inter-satellite geometry would be available. These data, the telemetered data, and ionospheric activity data derived from vertical soundings and other sources would be used to study the various aspects of ionospheric propagation. The experiment would also provide signals which might be used by other scientific organizations to study the many space-to-ground propagation phenomena which have been the subject of considerable theoretical study but little experimental work.

3.3.2 Concept 2

The P-11 experiment, unlike the "zombie" concept discussed above, would be reasonably well defined in advance insofar as inter-satellite geometry is concerned. The Agena

orbit would vary as previously noted, and the P-11 would enter a circular orbit at an altitude of about 200 nm; the two orbits would be co-planer. Because of the different periods to the orbits, the two vehicles would separate quite rapidly and soon be separated by 11,000 nm. Upon reaching maximum separation, the range between the satellites would close, and the cycle would then begin anew. It is readily understood that this geometry is considerably less complex than that involved in the "zombie" experiment. The transmitting P-11 would last at least six months and thus could be used by a number of receiving satellites, allowing considerable flexibility of operation.

The extreme range involved requires that the experiment resemble the "zombie" experiment in many respects. The fact that the P-11 would remain above the peak of the F_2 layer makes it desirable to have the lower frequency somewhat lower than that proposed for the "zombie" so that some details of the upper "side" of the ionosphere might be studied when the vehicles are close together. To perform such measurements the lower frequency should be close to the critical frequency of the ionosphere; 4 to 5 Mc would probably be the frequency range involved.

The contents of the transmitting and receiving packages would be essentially the same as those previously described, except for changes due to the different low frequency to be used in the P-11 configuration and such changes in sequencing as are deemed necessary. The transmitting antennas might have to be separate from the transmitter package, and the power for the transmitters would be derived from the P-11's solar cells; but operation of the equipment, recovery of the data, and the weights would be as proposed for the "zombie" experiment.

3.3.3 Concept 3

This concept involves a sub-satellite designed to separate from a Program 162 vehicle, carrying with it the transmitting package. The sub-satellite would contain its own power supply and a beacon for tracking purposes, and for technical reasons, would separate from the Agena at a very low velocity. The mother vehicle would have the same orbit discussed previously and because of the low separation velocity, the sub-satellite would have essentially the same orbit as the mother vehicle.

Because of the orbit eccentricity, the two satellites would operate above, in, and below the maximum of the F_2 layer at rather short ranges. It is, therefore, suggested that the experiment should study ducting, ionospheric attenuation, pulse-shape distortion (frequency dispersion), ionospheric reflection, etc. For those purposes it appears best to operate at frequencies of 7 and 14 Mc.

The transmitting sub-satellite would include the components discussed, plus batteries and ejection-spin mechanism. The receiving package would be the same as in the other concepts. The transmitting satellite will weight at least 50 lb and the receiving package will weigh about 15 lb.

Only the Agena would be tracked by the Air Force telemetry stations; the services of SPADETS and similar organizations would be enlisted to track the ejected satellite. Acquisition of the experimental data would be the same as the other concepts, and auxiliary scientific studies could be performed as previously described.

3.4 EXPERIMENT SELECTION

It is necessary, as part of the preliminary design, that the type of experiment to be performed be determined. The preceding section has discussed the experiments possible within the Program 162 framework. The relative advantages and disadvantages of these approaches are presented below for comparison.

3.4.1 Zombie to Zombie

Advantages:

(1) The weight penalty per Agena is a minimum for this concept.
(2) The possibility of obtaining vehicle space is quite high.
(3) The costs of the experimental packages are about the same as for P-11 and less than the sub-satellite.
(4) A wide range of inter-satellite geometries can be anticipated.
(5) The experimental life would be roughly three weeks.

Disadvantages:

(1) The experimental geometry is very complex and data reduction will thus be complicated.
(2) The probability of experiment success is possibly slightly lower than for the other concepts.
(3) The radiation from the transmitters might present a very serious RFI problem for the other experiments on board.
(4) There is no way at present to assure that the two Agenas would be launched sequentially; therefore, it is possible that both launches would be successful but so far apart in time as to preclude cooperation between vehicles.

3.4.2 P-11 to Agena

Advantages:

(1) This concept is only slightly heavier in total weight than the Zombie experiment.
(2) Costs of the experimental packages are about the same as Zombie and less than the sub-satellite.
(3) The geometry is less complex than for the Zombies and yields the greatest possible separation.
(4) The transmitter can operate for up to six months and thus may be used with a number of receiving satellites.

Disadvantages:

(1) There are only a few P-11s planned and space has been fully assigned; therefore, it is unlikely that the experiment could be flown unless another experiment fails to materialize or is cancelled.
(2) Flights on P-11 must pay a weight-proportional share of the cost of the P-11.
(3) RFI might be a severe problem aboard the P-11.

3.4.3 Sub-Satellite to Agena

Advantages:

(1) The geometry is simpler than for the other concepts and is very precisely controlled.
(2) The experiment is less likely to malfunction than the other experiments.

Disadvantages:

(1) The weight is greater because of the batteries.
(2) The cost of the experimental packages would be slightly higher than for the other experiments.
(3) The experimental life of the ejected capsule would be roughly one week.

While each configuration presents interesting possibilities, certain of the practical difficulties or simplicities must dominate in the selection of the optimum course of action:

(1) The "zombie to zombie" concept must be discarded for the reasons given in disadvantages (3) and (4) above. While RFI might be eliminated, the possibility of getting the two packages into orbit within several weeks of each other is too small to be seriously considered for this type of operation.
(2) The "P-11 to Agena" concept must at the present time be discarded because of disadvantages (1), (2), and (3) listed above. Again, while RFI might be eliminated, the cost of the P-11 could be as high as $250,000 and, at present, all P-11's scheduled to be flown are completely filled.
(3) The "sub-satellite to Agena" concept appears to be the most likely candidate. However, although this approach has two very strong advantages, as listed above, the precise control of experimental geometry would be of particular importance in the reduction of data.

Therefore the "sub-satellite to Agena" concept is recommended for immediate implementation.

3.5 EXPERIMENTAL DESIGN

The effects of the ionosphere upon the transmission between satellites will depend upon the geometric relationship between the two satellites and the ionosphere. Calculation of this relationship for a large number of points between the start and the end of the experiment would be expensive and wasteful; therefore, an approximate technique was applied which yields a rough solution above a given altitude. This technique involves finding the time from separation required for the line of sight (from the mother vehicle at apogee to the sub-satellite) to become tangent to an ionospheric layer. The mathematical equations used to calculate these data are derived in Appendix A, which includes the symbols employed and the Fortran program used. (It should be noted that the solutions obtained are exact; the use to which these solutions will be put in the following yields the rough solution referred to above.) Figure 3-1, derived from Fig. A-3 of Appendix A, shows the time required for occultation of the inter-vehicular line of sight by the 160-nm layer of the ionosphere when the mother vehicle is at apogee. This graph is almost correct for the case in which the sub-satellite is at apogee, because of the small difference in the orbital parameters. If it is desired to find the time of occultation for altitudes of the mother vehicle other than apogee, this figure may be used as follows to obtain an approximate answer. Given the initial velocity increment parallel to the flight path (for an increment given at perigee), enter the graph at the time of interest and read the altitude from the apogee scale. This is the rough altitude of the vehicle nearest apogee (when both vehicles are on the same side of apogee) at the time of occultation by the 160-nm layer. The reverse procedure can be used to find the time of first occultation when both vehicles are on the same side of apogee and the altitude of the vehicle nearest apogee is given. No estimate of the error involved has been made, but the percentage error obviously is small when both trajectories have a low apogee.

It is also desirable to be able to compute the inter-satellite distance without resorting to a computer, but it would appear that this is quite difficult to do since the altitude

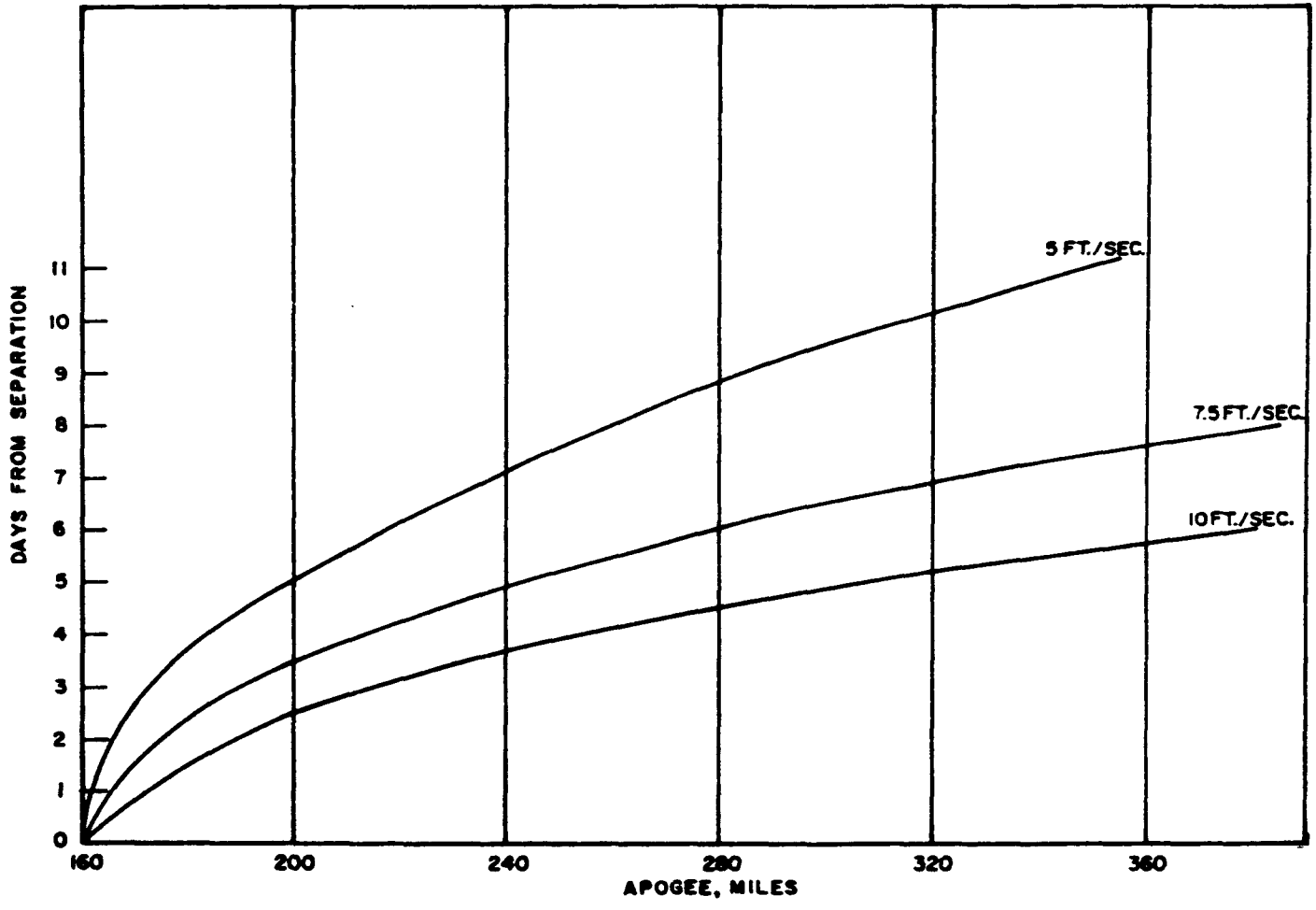

Fig. 3-1 Time to Occultation by 160-nm Layer for Flight Path Velocity Increment Given

varies from 115 nm to as high as 380 nm. It is shown in Appendix B however, that the distance between satellite is given within 8 percent by

$$d = \sqrt{a_1^2 + a_2^2 - 2a_1a_2\cos\theta_d} \tag{3.1}$$

where

- d = distance between satellites
- a_1 = semi-major axis length of first orbit
- a_2 = semi-major axis length of second orbit
- θ_d = earth-centered angle between vehicles

and the eccentricities of both orbits are under 0.035; this means that for a perigee of 115 nm, the apogee is less than 245 nm. Such an apogee is quite probable for Agena flights. Equation 3.1 may be rewritten as

$$d = a\sqrt{2 - 2\cos 2\pi\left(\frac{1}{T_2} \quad \frac{1}{T_1}\right)t} \tag{3.1A}$$

where

- a = semi-major axis of the mother satellite
- T_1 = period of sub-satellite
- T_2 = period of mother satellite
- t = time from the first apogee following ejection

The reason for taking t, above, from the time of first apogee is the fact that forward ejection actually increases the orbital period; therefore, the ejected package moves ahead of and rises above the mother vehicle until apogee, at which time it is above the mother, but the mother has caught up and is passing underneath. For the range of altitudes under consideration here, the difference in orbital period is 1.5×10^{-3} hr or 5.4 sec for an initial separation velocity of 7.5 fps. At perigee at the end of the

first orbit following ejection, the interval between vehicles will be 2.7 sec or 11.5 nm, with the mother now preceding the sub-satellite. Given the 7.5 fps velocity increment at separation, the altitude difference at apogee will be 4.7 nm for all altitudes in the range under consideration.

The transmitter structure will consist of the transmitter shell and internal bracketery, intermediate support structure, and four primary support fittings. The shell will be attached to the Agena primary structure by means of the four primary fittings and pyrotechnic pin-puller assemblies. The intermediate support structure is to be attached to the equipment rack with bolts. The release mechanism and impulse spring assembly will be integral with the intermediate support structure and the spring assembly is to be actuated with a pin puller.

Ejection and spin will be accomplished by pivoting the package about one end and releasing after 90 deg of rotation. A spring system will produce an initial tangential release velocity of 7.5 fps and a spin rate of 1.4 rev/sec. A diagram of the ejection-spin up operation is given in Fig. 3-2. The antennas are to be erected at a rate of .045 fps, assuring an ample safety factor for theoretical loads. However, it is planned to test the antenna to determine its maximum moment of inertia. After release, the package will be spinning about the axis of maximum mass moment of inertia, and due to antenna erection, the mass moment of inertia will increase by a factor of 20.3 in the plane of rotation. The terminal spin rate will be .06 rev/sec. These parameters are deemed satisfactory for a stable configuration.

A preliminary thermodynamic analysis of the ejected package was performed on the basis of preliminary design data and is detailed in appendix C. The mean vehicle temperature was calulated for a variety of absorptivity-to-emissivity ratios, for two spin orientations, and for several launch times. The spin orientation chosen in the preliminary design (spin axis perpendicular to earth's surface at perigee) proves to be close to optimum for a wide range of launch times. It will be necessary to select a ratio of α/ϵ (absorptivity to emissivity) that is suitable for all launch times;

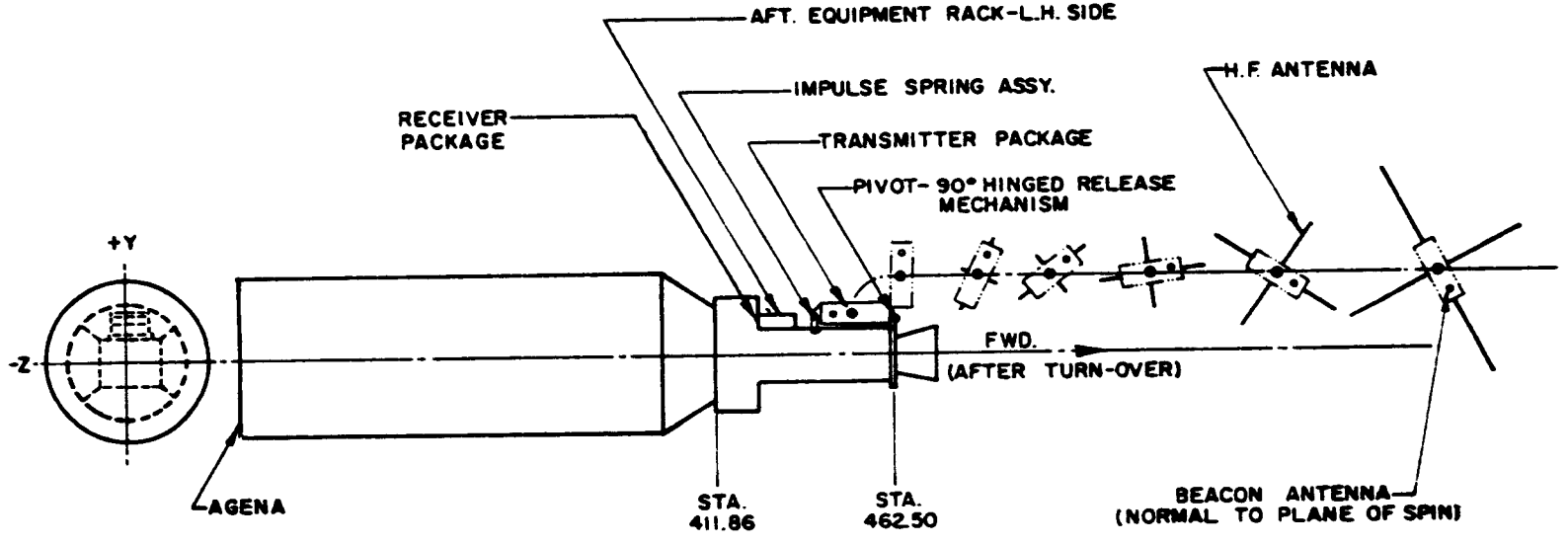

Fig. 3-2 Satellite-to-Satellite Propagation Experiment

but, for the temperature range desired for the equipment, the mean temperature would lie within a 22°F range. A sample computer calculation showed that internal major component temperatures will probably vary about 12°F above and below the mean temperature. Thus, the internal temperature may be controlled within moderate bounds by the simple expedient of varying the α/ϵ ratio.

Section 4
SUMMARY

The effects of the ionosphere upon electromagnetic radio-frequency radiation have been discussed. Numerical examples of attenuation, Faraday effect, pulse dispersion, and dispersive Doppler have been given. It was shown that attenuation would become significant at long ranges (1,000 nm or so), Faraday effects would be detectable within a few minutes, pulse shape deformation can be quite drastic at ranges of 40 nm or less, and the dispersive Doppler effect is so small as to be virtually unmeasurable.

Two basically different approaches to ionospheric studies were presented, the sounding technique and a phenomenological approach, and it was indicated that the latter was more in keeping with satellite operations. Several classes of experimental geometries were discussed, as were the experiments possible with each and some of the more serious attendant problems.

Details of the Government-furnished equipment were given, and the three possible modes of operation within the limits of Program 162 were described in detail. After a consideration of all factors, it was decided that the experiment could be performed only as originally envisioned, with ejection of a small, transmitting satellite from the Agena. Details of the orbital geometry were calculated, and an acceptable method of achieving ejection and spin was designed. Thermal calculations were performed to assure that internal temperatures could be maintained so as not to exceed equipment design limits.

Appendix A

LINE-OF-SIGHT OCCULTATION BY ATMOSPHERIC LAYER

In conjunction with the proposed experiment investigating radio propagation between earth satellites, it was necessary to determine the time required to achieve occultation by an ionospheric layer of the line of sight between a mother and an offspring satellite. It seemed advisable to consider the problem in its most general form and to specialize to the particular problem only in the last steps. Accordingly, the relationship was found between the original orbital parameters, an arbitrary velocity increment given to the satellite, and the resultant orbital parameters – the only restrictive assumptions being that the velocity increment is taken as impulsive and that the earth's gravity field is taken to be that resulting from a point mass. From the geometry of the system of satellites and earth, a family of configurations was found at which occultation can occur -- assuming the major axes of the mother and offspring orbits are coincident and that the mother is at apogee when occultation occurs. Finally, a computer program was written and run to find the time to occultation for various mother satellite orbits using the results from above and assuming the entire (small) velocity increment to be along the flight path. The program computes the time from incrementation until the satellites have relative positions such that occultation will occur the next time the mother satellite passes its apogee – not necessarily the time from incrementation to the first occultation. The parameters studied are: apogee and perigee height of the mother satellite; incrementation velocity, and position in orbit at which the velocity is incremented. The computer output includes: mother satellite period; offspring period; mother satellite orbit semi-major axis, eccentricity, and apogee height; and the "Time to Occultation."

LIST OF VARIABLES*

a semi-major axis of ellipse

e eccentricity of ellipse

---

*See Fig. A-1

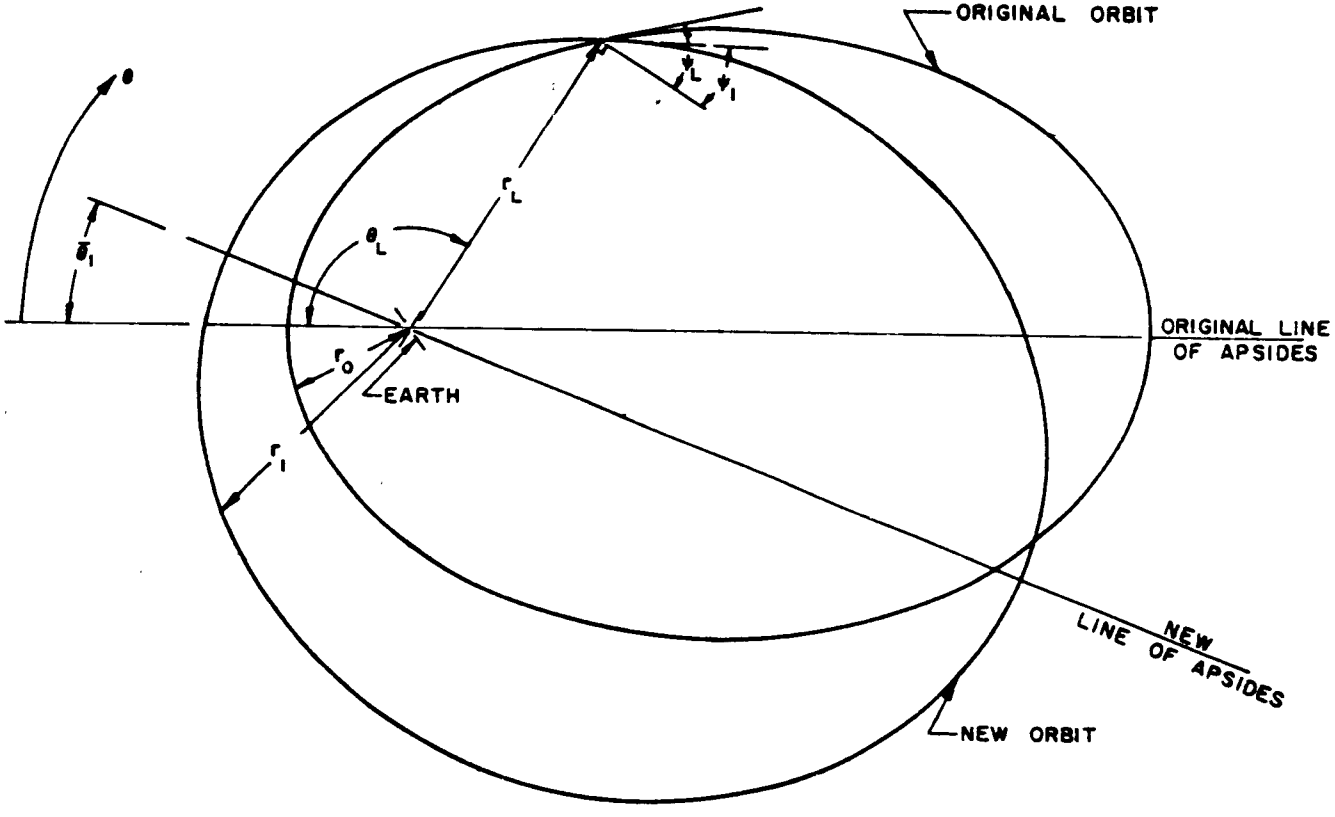

Fig. A-1 Orbit Variables

g acceleration due to gravity at earth's surface

K special grouping of variables $-\sqrt{\mu/a(1 - e^2)}$

P dimensionless velocity $- v \sqrt{\frac{a}{\mu}}$

q special grouping of variables $- \frac{e \sin \theta}{1 + e \cos \theta}$

r focus to orbit distance $- a(1 - e^2)/1 + e \cos \theta$

R mean radius of earth

S special grouping of variables $-\sqrt{\frac{1 + e^2 + 2e \cos \theta}{1 - e^2}}$

T period of satellite orbit

v velocity increment imparted to satellite

V velocity of satellite $\sqrt{\frac{\mu}{a(1 - e^2)}} \sqrt{1 + e_o^2 + 2e_o \cos \theta_o}$

α angle between velocity increment and original velocity

β angle between velocity-velocity increment plane and orbital plane

γ angle between original and final orbital planes

θ angular distance from perigee

μ gravitational constant of earth $- gR^2$

ψ angle between velocity vector and normal to radial line from occupied focus to satellite.

SUBSCRIPTS

o original orbit

1 offspring orbit or 1-axis component

2 2-axis component

3 3-axis component

L value of variable when velocity increment is given

Define the 1, 2, 3 coordinate system as follows: the 1 axis lies along the velocity vector in the original orbit; the 2 axis lies normal to 1 in the plane of the original

orbit with the positive sense in the direction of increasing orbital altitude; the 3 axis lies perpendicular to the plane of the orbit with positive sense such that 1, 2, and 3 form a right-handed coordinate system.

ψ is the angle between the radial line and the 2 axis-positive when the velocity has a positive radial component.

Choose the angles α and β such that an arbitrary line, PQ, is defined by them in the following way: α is the angle between the 1 axis and PQ – 0 deg $\leq \alpha \leq$ 180 deg – and β is the angle between the 1-PQ and the 1-2 planes – - 180 deg $< \alpha \leq$ 180 deg

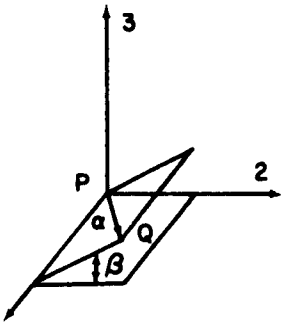

If a velocity increment v is given to the satellite, denoting the values of r, θ, V, and ψ at this time by the subscript L:

$$V_{11} = V_{L1} + v_1 = V_L + v \cos \alpha$$

$$V_{12} = V_{L2} + v_2 = v \sin \alpha \cos \beta$$

$$V_{13} = V_{L3} + v_3 = v \sin \alpha \sin \beta$$

and

$$V_1^2 = V_L^2 + v^2 + 2V_L\, v \cos \alpha \qquad \text{(A.1)}$$

The new orbital plane lies at an angle γ to the original plane determined by $\tan \gamma = V_{13}/V_{1P}$ – where V_{1P} is the velocity in the 1, 2 plane perpendicular to the radius, thus:

$$\tan \gamma = \frac{v \sin \alpha \sin \beta}{V_L \cos \psi_L + v \cos \alpha \cos \psi_L - v \sin \alpha \cos \beta \sin \psi_L} \qquad \text{(A.2)}$$

The new velocity vector makes an angle $\psi_1 = \arcsin V_{1R}/V_1$ with the perpendicular to the radius, thus

$$\sin \psi_1 = \frac{V_L \sin \psi_L + v \cos \alpha \sin \psi_L + v \sin \alpha \cos \beta \cos \psi_L}{(V_L^2 + v^2 + 2V_L v \cos \alpha)^{1/2}} \qquad \text{(A.3)}$$

For an orbit with semi-major axis a_o, eccentricity e_o, and its perigee located at $\theta_o = 0$, if $\mu \equiv gR^2$

$$\tan \psi_o = \frac{e_o \sin \theta_o}{1 + e_o \cos \theta_o} \qquad \text{(Ref. 4)} \qquad \text{(A.4)}$$

and

$$V^2 = \frac{\mu}{a_o(1 - e_o^2)} \left[1 + e_o^2 + 2e_o \cos \theta_o\right] \quad \text{(by implication) (Ref. 4)} \qquad \text{(A.5)}$$

Thus, since $V_{circ} \equiv \sqrt{\mu/a_o}$: (Ref. 4)

$$V_{max}^2 = V_{circ}^2 \frac{(1 + e)^2}{(1 - e^2)} = \frac{1 + e}{1 - e} V_{circ}^2$$

$$V_{min}^2 = V_{circ}^2 \frac{(1 - e)^2}{(1 - e^2)} = \frac{1 - e}{1 + e} V_{circ}^2 = \left(\frac{1 - e}{1 + e}\right)^2 V_{max}^2$$

Furthermore:

$$r_o = \frac{a_o\left(1 - e_o^2\right)}{1 + e_o \cos \theta_o} \qquad \text{(Ref. 4)} \qquad \text{(A.6)}$$

When r, V, and ϕ are known, the orbital parameters a, e, and θ may be found from:

$$a = \frac{r}{2 - rV^2/\mu} \quad \text{from} \quad V^2 = \mu\left(\frac{2}{r} - \frac{1}{a}\right) \qquad \text{(Ref. 4)} \qquad \text{(A.7)}$$

$$e = \sqrt{1 - \frac{rV^2}{\mu}\left(2 - \frac{rV^2}{\mu}\right)\cos^2\phi} \qquad \text{(Ref. 3 or 4) (by implication)} \qquad \text{(A.8)}$$

and

$$\cot\theta = \cot\phi\left(1 - \frac{\mu}{rV^2\cos^2\phi}\right) \qquad \text{(Ref. 2)} \qquad \text{(A.9)}$$

Thus, if the velocity increment v is given at $\theta = \theta_L$, using relations (A.4 and A.5) with Eqs. (A.1, 2, and 3) gives:

$$V_1^2 = K_o^2\left(1 + e_o^2 + 2e_o\cos\theta_L\right) + v^2 + 2vK_o\cos\alpha\sqrt{1 + e_o^2 + 2e_o\cos\theta_L} \qquad \text{(A.10)}$$

where

$$K_o \equiv \sqrt{\frac{\mu}{a_o\left(1 - e_o^2\right)}} \qquad \text{(A.11)}$$

while

$$\tan\gamma = \frac{v\sin\alpha\sin\beta}{K_o(1 + e_o\cos\theta_L) + \dfrac{v\cos\alpha(1 + e_o\cos\theta_L)}{\sqrt{1 + e_o^2 + 2e_o\cos\theta_L}} - \dfrac{e_o v\sin\alpha\cos\beta\sin\theta_L}{\sqrt{1 + e_o^2 + 2e_o\cos\theta_L}}} \qquad \text{(A.12)}$$

and

$$\sin \psi_1 = \frac{K_o e_o \sin \theta_L + \dfrac{e_o v \cos \alpha \sin \theta_L}{\sqrt{1 + e_o^2 + 2e_o \cos \theta_L}} + \dfrac{v \sin \alpha \cos \beta \left(1 + e_o \cos \theta_L\right)}{\sqrt{1 + e_o^2 + 2e_o \cos \theta_L}}}{\left[K_o^2 \left(1 + e_o^2 + 2e_o \cos \theta_L\right) + v^2 + 2vK_o \cos \alpha \sqrt{1 + e_o^2 + 2e_o \cos \theta_L}\right]^{1/2}}$$

(A. 13)

from relations (A. 6, 7, 8, and 9), since

$$\frac{r_o V_1^2}{\mu} = \frac{1 + e_o^2 + 2e_o \cos \theta_L + \left(\frac{v}{K_o}\right)^2 + 2 \frac{v}{K_o} \cos \alpha \sqrt{1 + e_o^2 + 2e_o \cos \theta_L}}{1 + e_o \cos \theta_L}$$

$$\left(2 - \frac{r_o V_1^2}{\mu}\right) = \frac{\left(1 - e_o^2\right)\left[1 - \dfrac{v^2 a_o}{\mu} - 2 \cos \alpha v \sqrt{\dfrac{a_o}{\mu}} \sqrt{\dfrac{1 + e_o^2 + 2e_o \cos \theta_L}{1 - e_o^2}}\right]}{1 + e_o \cos \theta_L}$$

(A. 14)

and

$$\frac{r_o V_1^2 \cos^2 \psi_1}{\mu} = (1 + e_o \cos \theta_L)\left[1 + 2v \sqrt{\frac{a_o}{\mu}} \frac{\cos \alpha - e_o \sin \alpha \cos \beta \dfrac{\sin \theta_L}{1 + e_o \cos \theta_L}}{\sqrt{\dfrac{1 + e_o^2 + 2e_o \cos \theta_L}{1 - e_o^2}}} + \frac{v^2 a_o}{\mu}\left\{\frac{1 + \left(\dfrac{e_o \sin \theta_L}{1 + e_o \cos \theta_L}\right)^2 - \left(e \cos \alpha \dfrac{\sin \theta_L}{1 + e_o \cos \theta_L} + \sin \alpha \cos \beta\right)^2}{\left(\dfrac{1 + e_o^2 + 2e_o \cos \theta_L}{1 - e_o^2}\right)}\right\}\right]$$

(A. 15)

$$a_1 = \frac{a_o}{1 - \frac{v^2 a_o}{\mu} - 2 \cos \alpha v \sqrt{\frac{a_o}{\mu}} \sqrt{\frac{1 + e_o^2 + 2e_o \cos \theta_L}{1 - e_o^2}}} \tag{A.16}$$

Defining

$$P_L = v \sqrt{\frac{a_o}{\mu}} = v \sqrt{\frac{r_{P_o}}{\mu(1 - e_o)}} \qquad r_P = \text{perigee radius} \tag{A.17}$$

$$q_L \equiv \left(\frac{e_o \sin \theta_L}{1 + e_o \cos \theta_L} \right) \tag{A.18}$$

$$S_L \equiv \sqrt{\frac{1 + e_o^2 + 2e_o \cos \theta_L}{1 - e_o^2}} \tag{A.19}$$

Relations (A.14) and (A.15) become

$$\left(2 - \frac{r_o V_1^2}{\mu} \right) = \frac{1 - e_o^2}{1 + e_o \cos \theta_L} \left[1 - \left(P_L^2 + 2 P_L S_L \cos \alpha \right) \right] \tag{A.20}$$

and

$$\frac{r_o V_1^2 \cos^2 \psi_1}{\mu} = (1 + e_o \cos \theta_L) \left[1 + 2P_L \frac{\cos \alpha - q_L \sin \alpha \cos \beta}{S_L} + P_L^2 \left\{ \frac{1 + q_L^2 - (q_L \cos \alpha + \sin \alpha \cos \beta)^2}{S_L^2} \right\} \right] \tag{A.21}$$

Thus

$$a_1 = \frac{a_o}{1 - \left(P_L^2 + 2P_L S_L \cos \alpha\right)} \tag{A. 22}$$

The expressions for e_1 and θ_1 are not as near and simple. However, by calculating relations (A. 20) and (A. 21) by use of Eqs. (A. 17, 18, and 19) and computing cot ψ_1 by use of Eq. (A. 4), the values of e_1 and θ_1 may be readily determined.

Assuming that e_o and P_L are small leads to

$$q_L \approx e_o \sin \theta_L$$

$$S_L \approx 1 + e_o \cos \theta_L$$

Thus

$$\left(2 - \frac{r_o V_1^2}{\mu}\right) \approx (1 - e_o \cos \theta_L)\left[1 - 2P_L \cos \alpha(1 + e_o \cos \theta_L)\right]$$

and

$$\frac{r_o V_1^2 \cos^2 \psi_1}{\mu} \approx (1 + e_o \cos \theta_L)\left[1 + 2P_L(\cos \alpha - e_o \sin \alpha \cos \beta \sin \theta_L)(1 - e_o \cos \theta_L)\right]$$

Thus

$$a_1/a_o \approx 1 + 2P_L \cos \alpha(1 + e_o \cos \theta_L)$$

$$e_1 \approx \sqrt{e_o^2 + 2P_L e_o(2 \cos \alpha \cos \theta_L + \sin \alpha \cos \beta \sin \theta_L) + 4P_L^2 \cos^2 \alpha}$$

This equation was derived by using an approximation of actual e_1, assuming e_o and P_o to be small. The value of θ_1 would probably be much different from that predicted by a small-value approximation for e_o and P_o and for that reason will not be approximated here.

The period of the satellite is $T = 2\pi \sqrt{\frac{a^3}{\mu}}$. Thus

$$T_1/T_o = \sqrt{(a_1/a_o)^3} = \left(1 - P_L^2 - 2P_L S_L \cos \alpha\right)^{-3/2}$$

$$= \left[1 - \left(v^2 \frac{a_o}{\mu} + 2v_o \sqrt{\frac{a_o}{\mu}} \cos \alpha \sqrt{\frac{1 + e_o^2 + 2e_o \cos \theta_L}{1 - e_o^2}}\right)\right]^{-3/2}$$

$$\approx 1 + 3v_o \sqrt{\frac{a_o}{\mu}} \cos \alpha \sqrt{\frac{1 + e_o^2 + 2e_o \cos \theta_L}{1 - e_o^2}} \qquad \text{(A. 23)}$$

Thus, if all other variables are fixed, the greatest change in period will arise from giving the velocity increment at $\theta_o = 0$ (perigee), the least from giving the increment at $\theta = \pi$ (apogee).

It is interesting to note the small effect on the orbital parameters due to the component of the incremental velocity which does not lie parallel to the flight path. An intuitive explanation of this is that – so far as the component normal to the orbit is concerned – the gravity force vector has a component which points in such a direction that the satellite will be accelerated back toward the original orbital plane. The force due to this component is (nearly) proportional to the distance from the original orbital plane so simple harmonic motion occurs about the original orbital position and is superimposed on the old orbital motion. The oscillation has a period nearly equal to the orbital period so that the orbital plane is rotated but other effects are quite small.

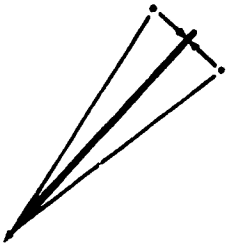

For a radial component – the difference $\mu/r^2 - v^2/r$ (the downward force) decreases as the satellite drops (assuming v = constant) and increases as the satellite rises

causing an acceleration back toward the original orbit. The period of the oscillation is nearly equal to the orbital period. Thus a radial increment causes a change in eccentricity with a small change in period.

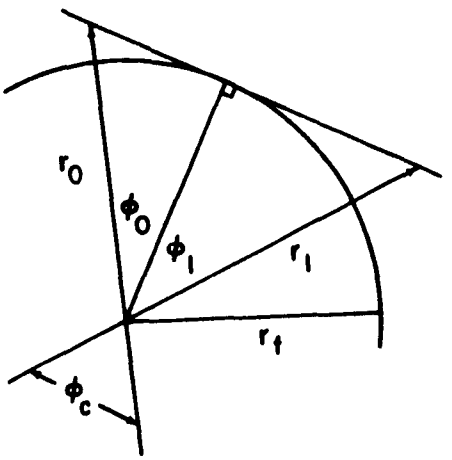

Defining $\rho_o \equiv \frac{r_o}{r_f}$; $\rho_1 \equiv \frac{r_1}{r_f}$ the normalized radii,

$$\rho_o = \sec \phi_o$$

$$\rho_1 = \sec \phi_1$$

Thus

$$\phi_c = \text{arc sec } \rho_o + \text{arc sec } \rho_1 = \text{arc cos } 1/\rho_o + \text{arc cos } 1/\rho_1$$

Taking

$$r_f = R + h_f$$

$$\rho_o = \frac{r_o}{R + h_f} \quad \text{and} \quad \rho_1 = \frac{r_1}{R + h_f}$$

If r_o is the apogee radius of the original orbit and $r_1 = a_1\left(1 - e_1^2\right)\Big/\left\{1 + e_1 \cos\left(\theta - \bar{\theta}_1\right)\right\}$

$$\rho_o = \frac{a_o(1 + e_o)}{R + h_f} \quad \text{and} \quad \rho_1 = \frac{a_1\ 1 - e_1^2}{R + h_f} - \frac{1}{1 + e_1 \cos\ (\theta - \bar{\theta}_1)} \qquad \text{(A.24)}$$

If ϕ_c is the angle from the line of apsides of the original orbit, θ is measured from the original orbit perigee, and $\bar{\theta}_1$ is the angle between the lines of apsides of the

two orbits: $(\theta - \bar{\theta}_1)_{crit.} = \pi + \phi_c - \bar{\theta}_1$ and

$$\rho_1 = \frac{a_1\left(1 - e_1^2\right)}{R + h_f} - \frac{1}{1 - e_1 \cos\ (\phi_c - \bar{\theta}_1)}$$

$$= P_1\ 1/1 - e_1 \cos\ (\phi_c - \bar{\theta}_1)$$

when

$$\dot{P}_1 \equiv \frac{a_1\left(1 - e_1^2\right)}{R + h_f} \tag{A.25}$$

now

$$\cos\ \phi_c = \cos\left[\text{arc cos}\ 1/\rho_o + \text{arc cos}\ \frac{1 - e_1 \cos\ (\phi_c - \bar{\theta}_1)}{P_1}\right]$$

But from trigonometry:

$$\cos\ (a + b) = \cos\ a \cos\ b - \sin\ a \sin\ b$$

Thus

$$\cos\ \phi_c = \frac{1}{\rho_o} \cdot \frac{1 - e_1 \cos\ (\phi_c - \bar{\theta}_1)}{P_1} - \frac{\sqrt{\rho_o^2 - 1}}{\rho_o} \frac{\sqrt{P_1^2 - \left(1 - e_1 \cos\left[\phi_c - \theta_1\right]\right)^2}}{P_1}$$

$$\rho_o P_1 \cos\ \phi_c + e_1 \cos\ (\phi_c - \bar{\theta}_1) - 1 = - \sqrt{\rho_o^2 - 1}\ \sqrt{P_1^2 - \left(1 - e_1 \cos\left[\phi_c - \bar{\theta}_1\right]\right)^2}$$

(A.26)

Since solution of this for general $\bar{\theta}_1$ would be very difficult and since in the problem under consideration $\bar{\theta}_1$ is almost zero. it will be assumed to be so, then

$$\left(\rho_o P_1 + e_1\right)\cos\phi_c - 1 = -\sqrt{\rho_o^2 - 1}\,\sqrt{P_1^2 - \left(1 - e_1\cos\phi_c\right)^2} \qquad \text{(A.27)}$$

from which

$$\left[\left(\rho_o P_1 + e_1\right)^2 + e_1^2\left(\rho_o^2 - 1\right)\right]\cos^2\phi_c - 2\left[\left(\rho_o P_1 + e_1\right) + e_1\left(\rho_o^2 - 1\right)\right]\cos\phi_c + \left[1 - \left(\rho_o^2 - 1\right)\left(P_1^2 - 1\right)\right] = 0$$

thus

$$\cos\phi_c = \frac{\left(\rho_o P_1 + e_1\right) + e_1\left(\rho_o^2 - 1\right)}{\left(\rho_o P_1 + e_1\right)^2 + e_1^2\left(\rho_o^2 - 1\right)} \pm \sqrt{\left[\frac{\left(\rho_o P_1 + e_1\right) + e_1\left(\rho_o^2 - 1\right)}{\left(\rho_o P_1 + e_1\right)^2 + e_1^2\left(\rho_o^2 - 1\right)}\right]^2 - \frac{1 - \left(\rho_o^2 - 1\right)\left(P_1^2 - 1\right)}{\left(\rho_o P_1 + e_1\right)^2 + e_1^2\left(\rho_o^2 - 1\right)}} \qquad \text{(A.28)}$$

The plus sign corresponds to the case when both radial lines are on the same side of the point of tangency so the minus sign gives the answer desired.

The time equation is

$$t - t_o = \sqrt{\frac{a^3}{\mu}}\left[\arcsin\left(\sqrt{1 - e^2}\,\frac{\sin\theta}{1 + e\cos\theta}\right) - e\sqrt{1 - e^2}\,\frac{\sin\theta}{1 + e\cos\theta}\right]\Bigg|_{\theta_{10}}^{\theta_{20}}$$

Thus, since $\theta = \pi + \phi_c - \bar{\theta}_1$ and $T = 2\pi\sqrt{\frac{a^3}{\mu}}$

$$\frac{t_c}{T_1} = \frac{1}{2\pi}\left[\arcsin\left\{\sqrt{1 - e_1^2}\,\frac{\sin(\phi_c - \bar{\theta}_1)}{1 - e_1\cos(\phi_c - \bar{\theta}_1)}\right\} + e_1\sqrt{1 - e_1^2}\,\frac{\sin(\phi_c - \bar{\theta}_1)}{1 - e_1\cos(\phi_c - \bar{\theta}_1)}\right]$$

(interpreting the arc sin as $-180° < \arcsin < 180°$) (A.29)

where t_c/T_1 is the fraction of the orbit through which the satellite must pass in going from $\theta = \pi - \bar{\theta}_1$ to $\theta = \pi + \phi_c - \bar{\theta}_1$. The number of hours after separation necessary for the offspring to have gained (or lost) this "distance" relative to the mother is given by

$$N = \frac{t_c}{T_1}\ (\text{orbits}) \Big/ \left|\frac{1}{T_1} - \frac{1}{T_o}\right| \left(\frac{\text{orbits}}{\text{hour}}\right)^* \qquad (A.30)$$

THE COMPUTER PROGRAM

The program utilizes the results of the analytical sections and is based on the following important assumptions:

1. The initial orbit is of small eccentricity.
2. The incrementation occurs near perigee or near apogee – i.e., not near $\theta = 90°$ or $270°$.
3. The ratio of the incremental velocity to the orbital velocity is small.
4. The component of the incremental velocity normal to the orbital flight path has only a negligible effect.
5. The line of apsides (major axis) of the orbit is not shifted by the incrementation.
6. The occultation occurs with the mother satellite at apogee.
7. The occulting layer is below the apogee heights of the satellite orbits.
8. "Time to Occultation" is the time from incrementation to the state at which occultation will occur the next time the mother satellite is at apogee.

*The orbital geometry is given in Fig. A-2 and the results of the calculation in Fig. A-3.

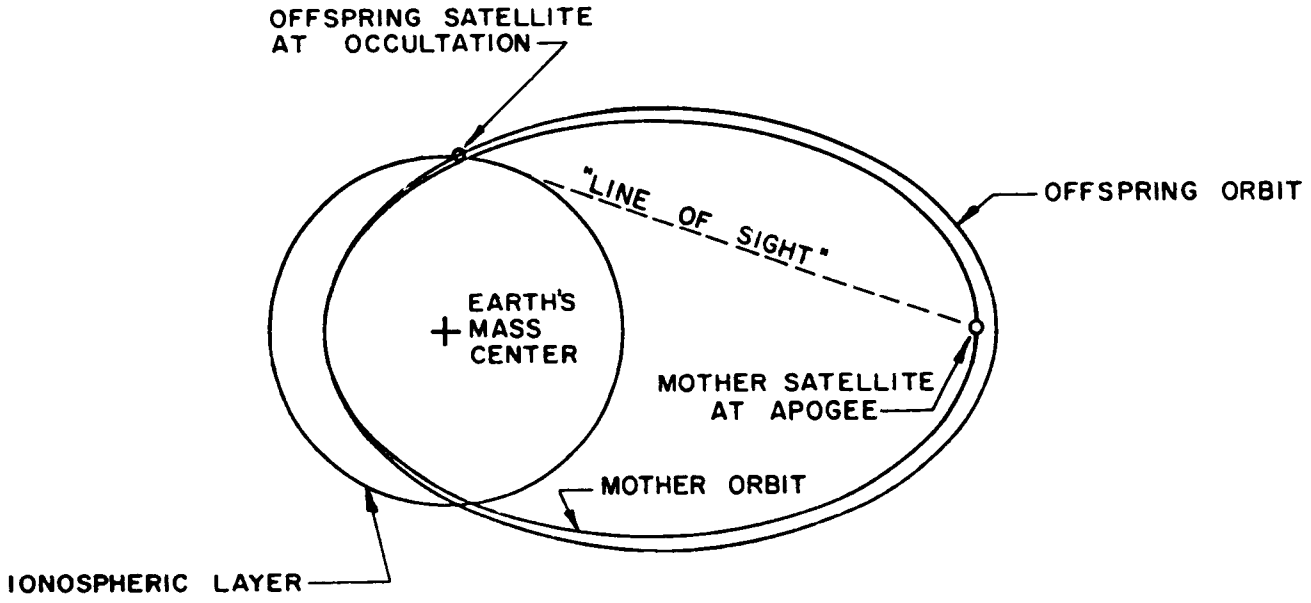

OCCULTATION OCCURS WHEN THE "LINE OF SIGHT" BETWEEN THE SATELLITES PASSES THROUGH THE IONOSPHERIC LAYER. IT WAS ASSUMED THAT THE MOTHER SATELLITE IS AT APOGEE WHEN OCCULTATION OCCURS.

Fig. A-2 Occulation Geometry

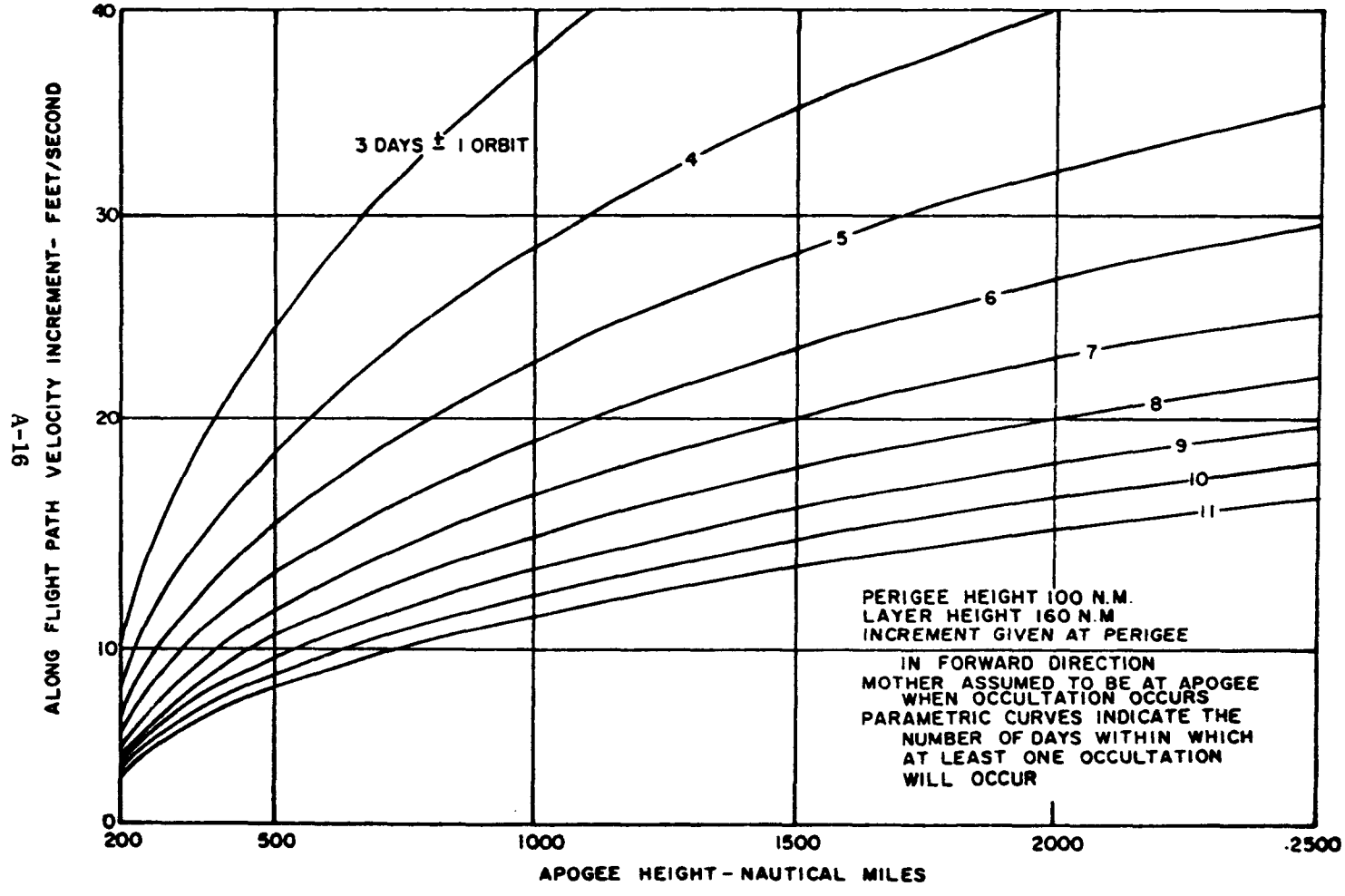

Fig. A-3 Satellite Temperature Variations

To use the computer program provide ALH (see the list of Fortran variables), PH, AHI, AH(1), TH(1), V(1), THI, VI, KA, KV, KT.

ALL DIMENSIONS IN NAUTICAL MILES

ALL SPEEDS IN FEET PER SECOND

ALL ANGLES IN RADIANS.

Fortran Variables

A(K)	Semi-major axis of mother orbit = a_o	(nautical miles)
AH(K)	Apogee height of mother orbit = h_a	(nautical miles)
AHI	Difference between successive mother orbit apogee heights	
ALH	Altitude of occulting atmospheric layer = h_f	(nautical miles)
B	Semi-major axis of offspring orbit = a_1	(nautical miles)
C	Differential cyclic frequency—mother to offspring	(orbits per hour)
CE	Cos (E - π)	
D	Eccentricity of offspring orbit = e_1	
E(K)	Eccentricity of mother orbit = e_o	
EE	Arc tan (sin E - π/cos E - π)	
EEE	E - π	
G	Gravitational constant = μ	
H	Approximate time to occultation	(hours)
J	Index variable on location in orbit at which velocity is incremented	
K	Index variable on mother orbit	
KA	Upper limit on value of K — thus number of orbits up to 25	

KT	Upper limit on value of J – thus number of locations for incrementation up to 6	
KV	Upper limit on value of L – thus number of incremental velocities up to 20	
L	Index variable on velocity increment	
P	Special constant = $P_1 = a_1(1 - e_1^2)/(R_e + h_f)$	
PH	Perigee Height = h_p	
Q	Special constant = $(\rho_o P_1 + e_1 + e_1 Z)/\left[(\rho_o P_1 + e_1)^2 + e_1^2 Z\right]$	
QA	Special constant = $(\rho_o P_1 + e_1)^2 + e_1^2 Z$	
R	Special constant = $\cos \phi_c$	
Ro	Special constant = $\rho_o = R_e + h_a/R_e + h_f$	
S	Sin E - π	
TB(J, K, L)	Period of offspring orbit = T_1	(hours)
TH(J)	Angle where increment is given = θ_I.	
THI	Difference between successive values of θ_L	
TM(K)	Period of mother orbit = T_o	(hours)
V(L)	Velocity increment along flight path = v cos α	(fps)
VI	Difference between successive velocity increments	
X	Special function = $2\sqrt{\frac{a_o}{\mu}}\sqrt{\frac{1 + e_o^2 + 2e_o \cos \theta_1}{1 - e_o^2}}$	
Y	Inverse of circular velocity = $\sqrt{\frac{a_o}{\mu}}$	
Z	Special constant = $z = \rho_o^2 - 1$	

```
      THIS IS A PROGRAM FOR DETERMINING THE PERIOD OF AN OFFSPRING
C  SATELLITE AND THE TIME NECESSARY FOR OCCULTATION OF THE LINE-OF-SIGHT
C  BETWEEN THE MOTHER AND OFFSPRING SATELLITES TO OCCUR. THE
C  PARAMETERS STUDIED ARE THE ORIGINAL ORBIT, THE ALTITUDE OF THE
C   OCCLUDING LAYER, THE ALONG-FLIGHT-PATH VELOCITY INCREMENT GIVEN TO
C  TO THE OFFSPRING, AND THELOCATION IN THE ORIGINAL ORBIT AT WHICH THE
C  INCREMENT IS GIVEN.  THIS NEGLECTS AIR DRAG, OBLATENESS OF THE
C  EARTH, AND ASSUMES THAT THE VELOCITY INCREMENT IS SMALL AND GIVEN
C IMPULSIVELY AND THAT THE ORIGINAL ORBIT IS OF SMALL ECCENTRICITY.
      DIMENSION TH(6),V(20),AH(25),A(25),E(25),TM(25),TB(25,6,20),H(25,6
     7,20),N(6)
      READ INPUT TAPE 5,10,ALH,PH,TH(1),AH(1),V(1),THI,AHI,VI,KA,KV,KT
   10 FORMAT(4E15.4/4E15.4,3I5)
      WRITEOUTPUTTAPE 6,10,ALH,PH,TH(1),AH(1),V(1),THI,AHI,VI,KA,KV,KT
      G=32.17*(3960.*5280.)**2/6076.1
   20 DO95K=1,KA
      A(K)=3440.+(AH(K)+PH)/2.
      E(K)=(AH(K)-PH)/(2.*3440.+AH(K)+PH)
      RO=(3440.+AH(K))/(3440.+ALH)
      Z=RO**2-1.
      Y=SQRTF(A(K)/G)
      TM(K)=2.*3.1415927*Y*A(K)*6.0761/3.6
   30 DO90J=1,KT
      X=SQRTF((1.+E(K)*(E(K)+2.*COSF(TH(J))))/(1.-E(K)**2))*Y**2.
   40 DO80L=1,KV
      TB(K,J,L)=TM(K)/((1.-V(L)*X)**1.5)
      B=A(K)/(1.-V(L)*X)
      C=((1.-V(L)*X)**1.5-1.)/TM(K)
      D=SQRTF(E(K)**2+4.*V(L)*Y*E(K)*COSF(TH(J))+4.*(V(L)*Y)**2)
      P=B*(1.-D**2)/(3440.+ALH)
      QA=(RO*P+D)**2+Z*D**2
      Q=(RO*P+D*(1.+Z))/QA
      R=Q-SQRTF(Q**2-(1.-Z*(P**2-1.))/QA)
      S=SQRTF((1.-D**2)*(1.-R**2))/(1.-D*R)
      CE=(D-R)/(1.-D*R)
      EE=ATANF(S/CE)
      IF(EE)50,50,60
   50 EEE=-EE
      GO TO 70
   60 EEE=3.1415927-EE
   70 H(K,J,L)=(EEE+S*D)/(6.2831853*ABSF(C))
      V(L+1)=V(L)+VI
      IF(V(L+1))80,75,80
   75 V(L+1)=V(L)+2.*VI
   80 CONTINUE
   90 TH(J+1)=TH(J)+THI
   95 AH(K+1)=AH(K)+AHI
      DO100I=1,KT
  100 N(I)=I
      DO190K=1,KA
      WRITEOUTPUTTAPE6,110,K,AH(K),K,A(K),K,TM(K),K,E(K)
  110 FORMAT(1H8,4H AH(I2,2H)=E12.4,5X,2HA(I2,2H)=E12.4,5X,3HTM(I2,2H)=E
     712.4,5X,2HE(I2,2H)=E12.4)
      WRITEOUTPUTTAPE6,120,(N(I),I=1,KT)
  120 FORMAT(1H0,10X,6(11X,3HTH(I1,1H)))
      WRITEOUTPUTTAPE6,130,(TH(I),I=1,KT)
```

```
THIS IS A PROGRAM FOR DETERMINING THE PERIOD OF AN OFFSPRING
  130 FORMAT(1H0,17X,(E12.4,4X))                                          590
      WRITEOUTPUTTAPE6,130,(K,N(I),I=1,KT)                                590
  140 FORMAT(2H0L,5X,4HV(L),2X,6(6X,5HTB(I2,1H,I1,3H,L)))                 610
      DO150L=1,KV                                                         620
  150 WRITEOUTPUTTAPE6,160,L,V(L),(TB(K,J,L),J=1,KT)                      630
  160 FORMAT(1H ,I2,1X,E12.4,2X,E12.4,(4X,E12.4))                         640
      WRITEOUTPUTTAPE6,170,(K,N(I),I=1,KT)                                650
  170 FORMAT(2H0L,5X,4HV(L),2X,6(7X,2HH(I2,1H,I1,3H,L)))                  660
      DO180L=1,KV                                                         670
  180 WRITEOUTPUTTAPE6,160,L,V(L),(H(K,J,L),J=1,KT)                       680
  190 CONTINUE                                                            690
      CALL EXIT                                                           710
      END(1,0,0,0,0,0,0,1,0,0,1,0,0,0,0,0,0)
```

Appendix A References

1. G. S. Gedeon, Advances in Astronautical Sciences, Vol. 3, Paper No. 19, Plenum Press, New York. 1958
2. E. T. Whittaker, Analytical Dynamics, Cambridge, 1961, pp. 87–90
3. V. G. Szebehely, Proceedings U. S. Third National Congress of Applied Mechanics. American Society of Mechanical Engineers, New York, 1958
4. K. Ehricke, Space Flight, Vol. I, Van Nostrand, New York, 1960 pp. 332–44

NOTE: The equations which refer to the sources may all be derived from the basic equations

$$r = \frac{a_o\left(1 - e^2\right)}{1 + e\cos\theta}$$

$$V^2 = \mu\left(\frac{2}{r} - \frac{1}{a_o}\right)$$

and

$$\tan\phi = \frac{1}{r}\frac{dr}{d\theta} = \frac{e\sin\theta}{1 + e\cos\theta}$$

all of which may be found in Ref. 4.

Appendix B

APPROXIMATION TO INTER-SATELLITE DISTANCE

If one knows the distance from each satellite to the center of the earth and the angle between the lines passing from the earth to the satellites, the distance between the satellites is found by the law of cosines to be

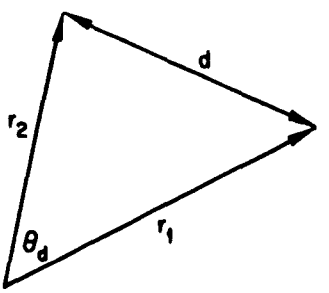

$$d^2 = r_1^2 + r_2^2 - 2r_1 r_2 \cos \theta_d$$

using the series for the inverse of the time equation as given by Moulton, et al., in Periodic Orbits, Washington, 1920 (pp. 55–59).

$$r_i = a_i \left\{ 1 - e_i \cos \omega_i t + \frac{e_i^2}{2} (1 - \cos 2\omega_i t) + \ldots\ldots \right\}$$

and

$$\theta_d = (\omega_2 - \omega_1)\, t + \left[- \left(2e_2 - \frac{e_2^3}{4} \right) \sin \omega_2 t - \left(2e_1 - \frac{e_1^3}{4} \right) \sin \omega_1 t \right] + \left[\frac{5e_2^2}{4} \sin 2\omega_2 t - \frac{5e_1^2}{4} \sin 2\omega_1 t \right] + \ldots\ldots$$

Thus

$$r_i^2 = a_i^2 + a_i^2 \left[- 2e_i \cos \omega_i t + e_i^2 (1 - \cos 2\omega_i t) \right.$$

$$- e_i^3 \cos \omega_i t (1 - \cos 2\omega_i t) + e_i^2 \cos^2 \omega_i t$$

$$\left. + \frac{e_i^4}{4} (1 - \cos 2\omega_i t)^2 + \ldots \right]$$

Since

$$\cos (a + b) = \cos a \cos b - \sin a \sin b$$

if

$$\Omega(t) \equiv \left(2e_2 - \frac{e_2^3}{4}\right) \sin \omega_2 t - \left(2e_1 - \frac{e_1^3}{4}\right) \sin \omega_1 t$$

$$+ \frac{5e_2^2}{4} \sin 2\omega_2 t - \frac{5e_1^2}{4} \sin 2\omega_1 t + \ldots\ldots$$

For

$$e_i \approx 0.035 \quad , \quad \Omega(t) \leq 0.10$$

thus

$$\cos \Omega(t) \approx 1.0$$

$$\sin \Omega(t) \approx \Omega(t)$$

Hence

$$\cos \theta_d = \cos (\omega_2 - \omega_1) t - \Omega(t) \sin (\omega_2 - \omega_1) t$$

and

$$d^2 = a_1^2 + a_2^2 - 2a_1a_2 \cos (\omega_2 - \omega_1) t + 2a_1a_2\Omega(t) \sin (\omega_2 - \omega_1) t$$

$$+ a_1^2 \left\{- 2e_1 \cos \omega_1 t + e_1^2(1 - \cos 2\omega_1 t) + e_1^2 \cos^2 \omega_1 t + \ldots.\right\}$$

$$+ a_2^2 \left\{- 2e_2 \cos \omega_2 t + e_2^2(1 - \cos 2\omega_2 t) + e_2^2 \cos^2 \omega_2 t + \ldots.\right\}$$

$$- 2a_1a_2 \left[\cos (\omega_2 - \omega_1) t - \Omega(t) \sin (\omega_2 - \omega_1) t\right] \left[- e_1 \cos \omega_1 t - e_2 \cos \omega_2 t\right.$$

$$\left. + e_1e_2 \cos \omega_1 t \cos \omega_2 t + \frac{e_1^2}{2} (1 - \cos 2\omega_1 t) + \frac{e_2^2}{2} (1 - \cos 2\omega_2 t) + \ldots.\right]$$

If

$$d^2 = a_1^2 + a_2^2 - 2a_1a_2 \cos (\omega_2 - \omega_1) t + \epsilon^2 a_1a_2$$

the error term ϵ^2 would not be expected to be larger than

$$\epsilon_M^2 = + 4(c_2 - e_1) + \frac{5}{2}\left(e_2^2 - e_1^2\right) + \left\{- 2c_1 + 3e_1^2\right\} + \left\{- 2e_2 + 3e_2^2\right\}$$

$$+ 2 \left[- e_1 - e_2 + e_1e_2 + e_1^2 + e_2^2\right] \approx - 8e_1$$

when

$$\cos\ (\omega_2 - \omega_1)\ t\ =\ 0$$

then

$$d^2\ =\ a_1^2 + a_2^2 + \epsilon^2 a_1\, a_2$$

if

$$a_1\ =\ a_2\ ,\quad d^2\ =\ (2 + \epsilon^2)a^2 =\ 1.72a^2$$

and since $d^2\ \approx\ 2a^2$

then

$$d_{actual}\ \approx\ 1.31a$$

$$d_{approx}\ \approx\ 1.41a$$

hence, the error is 8 percent or less if one says

$$d^2\ =\ a_1^2 + a_2^2 - 2a_1\, a_2 \cos\theta_d$$

or

$$d\ =\ \sqrt{a_1^2 + a_2^2 - 2a_1\, a_2 \cos\ (\omega_2 - \omega_1)t}\ ,\quad \text{if } e_1\ ,\ e_2\ \leq 0.035$$

Appendix C
PRELIMINARY THERMODYNAMIC ANALYSIS

The vehicle was assumed to be a box of .04-in. thick HM214-T8 magnesium 10 by 14 by 20 in. covering several internal equipment boxes. Total weight was assumed to be 50 lb, of which 5 lb was external structure. The equipment was assumed to have 2.6 w continuous power dissipation internally. The experiment was assumed injected into an orbit between $\beta = 0$ and $\beta = 45$ deg (60 to 64 percent sunlight) and to be spinning about its stable axis. The orbit was assumed to vary from 115 to 225 nm and was nearly polar. Calculations were performed for the cases of spin axis at parallel and spin axis perpendicular to the earth's surface when the satellite is perigee.

An analytical approximation of the mean orbital temperatures for the entire vehicle may be made utilizing time-averaged heat rates for the external surfaces and using different paint patterns with varying ratios.

The differential equation for satellite temperature (assuming the spin axis parallel to the earth surface at perigee) is:

$$\bar{c}\,\frac{dT}{d\theta} = \sum A\alpha fS + \sum A\alpha E_a + \sum A\epsilon E_s + P - \sum A\epsilon\sigma T^4 \qquad (C.1)$$

where

$\bar{c}$ = thermal capacity ~ Btu/° F

T = mean satellite temperature ~ °F

A = external surface area ~ ft^2

α = absorptivity

f = fraction of orbit in sunlight

S = solar constant ~ .123 Btu/sec-ft^2

ϵ = emissivity

E_s = earth radiation in infrared spectrum

E_a = earth reflection or albedo

P = power

σ = Stefan-Boltzman constant

θ = time

The maximum area that can be illuminated by the sun is 2.456 ft^2 and minimum is 1.505 ft^2.

The leading surface in orbit is 1.945 ft^2 and has average earth radiation of .007 Btu/ft^2-sec and average albedo of .00515 Btu/ft^2-sec in noon orbit and .00364 Btu/ft^2-sec in β = -45 deg orbit. These heat rates are symmetrical for the trailing edge. The circumference has 4.73 ft^2 of surface area and average earth radiation of .0068 Btu/ft^2-sec and albedo of .0049 Btu/ft^2-sec in a noon orbit with a value of .00347 Btu/ft^2-sec in β = -45 deg orbit.

In order to simplify the solution, it will be assumed that the outer paint surface α/ϵ ratio is varied for β^* = 0 and β = 45 deg. In β = 0 orbits, 60 percent of orbit is in sunlight and 64 percent is in sunlight for β = -45 deg. Substituting values in the equation, remembering that $\bar{c}\frac{dT}{d\theta} = 0$ in steady state, and making suitable modification to Eq. (C.1) gives:

β = 0 deg (MINIMUM ENERGY ORBIT, spin axis parallel to earth at perigee)

$$\sigma T^4 = .0179\ \alpha/\epsilon + .00689 \qquad \text{(C.2)}$$

---

*β = angle between earth-sun line and satellite orbital plane.

β = ± 45 deg (spin axis parallel to earth at perigee)

$$\sigma T^4 = .02597\ \alpha/\epsilon + .00689 \qquad \text{(C.3)}$$

β = 0 to β = ± 90 (spin axis passes through earth center at perigee)

$$\sigma T^4 = \left\{\frac{1.945 \cos\beta + 1.505 \sin\beta\ .123f + .005 \cos\beta}{8.62}\right\} \alpha/\epsilon + .00689 \qquad \text{(C.4)}$$

Equations (C. 1) and (C. 2) are plotted in Fig. C-1 and various α/ϵ values for Eq. (C. 3) are plotted in Fig. C-2.

In order to get typical time-temperature histories of the satellite, a small computer mathematical model was set up utilizing 4 nodes or equipment parts. Node 1 corresponded to the leading edge at perigee and Node 3 to the trailing edge at perigee. Node 2 represented the other external surfaces. Node 4 was the lumped interior equipment, including the transmitter.

Orbital heating rates were entered as time-dependent functions into external surfaces to account for solar illumination, earth reflection, and earth emission in the infrared spectrum. The internal power was delivered to the internal equipment node.

The vehicle interior was assumed to be one homogeneous structure of similar dimensions. External structure, internal surface, and internal box were painted with black Kemacryl to maximize internal radiative coupling. This will permit the 2.6 w to be transmitted to vehicle skin and to be rejected to space. This analysis assumed further that there was no convective or conductive heat transfer from vehicle interior to the surface. An α/ϵ ratio of 1.1:1 was used.

The most likely orbit is expected to be that where β = -45 deg with the solar vector inclined 38.5 deg to the spin axis. This was the case selected for analysis on the digital computer. The mathematical model then produced a time-temperature history of the equipment node and skin nodes showing the effects of entering and leaving earth's shadow and other orbital variations experienced by the vehicle.

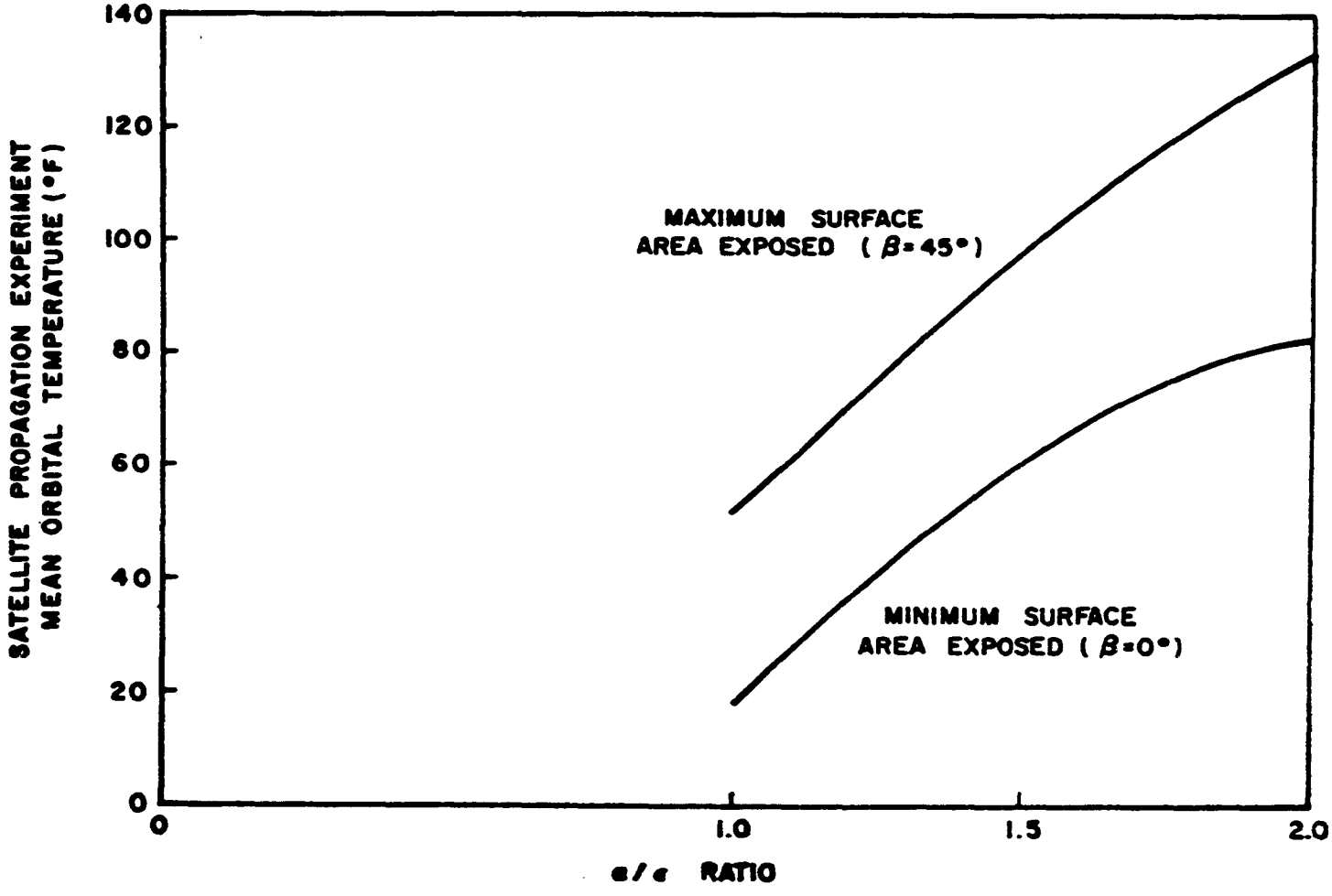

Fig. C-1 Mean Satellite Propagation Experiment Temperature (No Internal Power) as a Function of Other β's

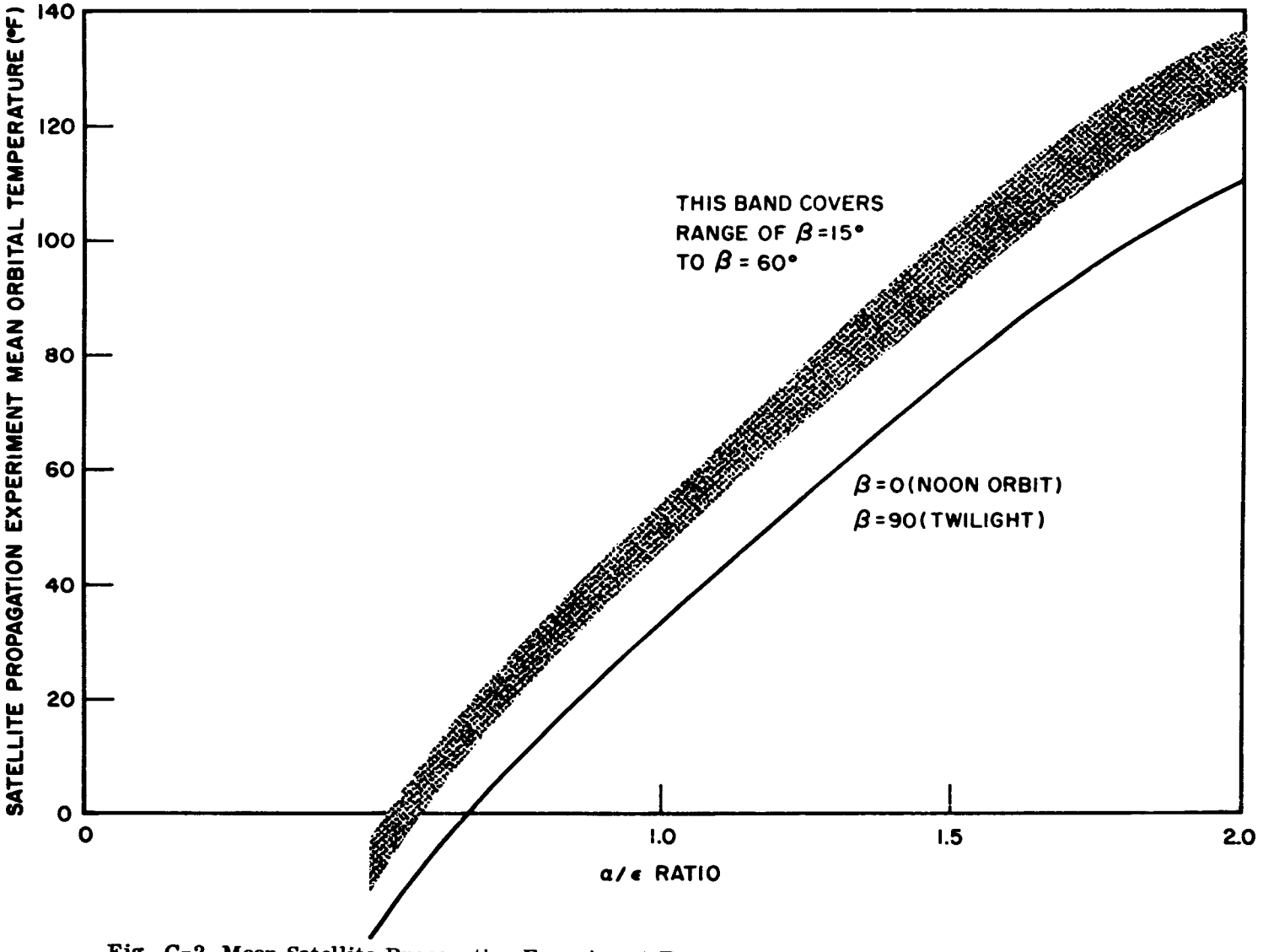

Fig. C-2 Mean Satellite Propagation Experiment Temperature (No Internal Power) Variation as a Function of β and α/ϵ Ratio. Spin Axis Assumed Perpendicular to Earth Surface at Perigee.

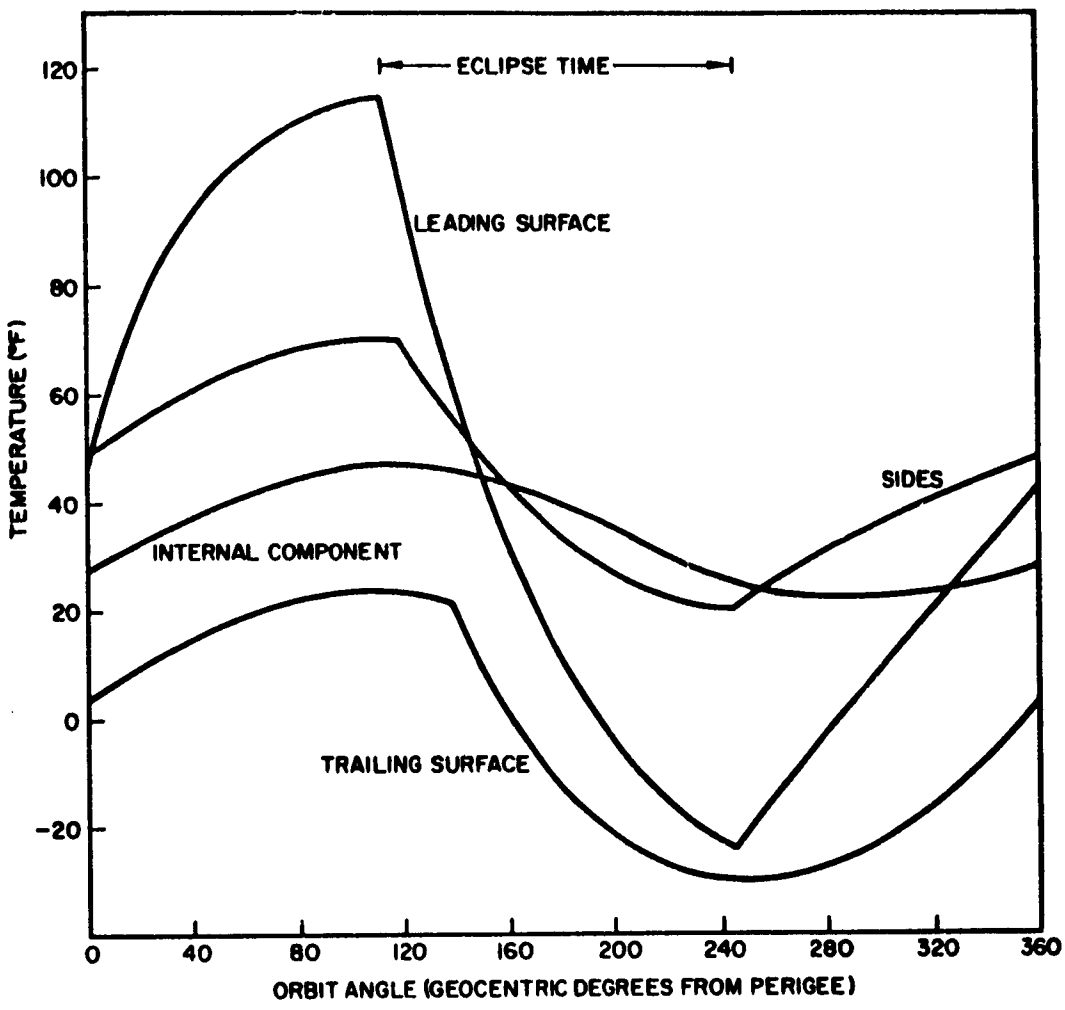

Fig. C-3 Satellite Temperature Variations

CONCLUSIONS

If the following conditions are furnished or established, the vehicle internal components can probably be maintained within temperature limits. First, excellent radiant coupling of interior components with external surfaces must be maintained. This is easily accomplished by selection of a high-emissivity paint. Also, with the expected complex internal structure, conductive heat transfer must be maximized so all component mountings should be carefully covered with a conducting silicone-type grease.

The internal power dissipation and sequence of events must be known very accurately. A mandatory requirement is precise definition of launch window, ejection time, dynamic history and final sun/satellite geometrical relationships.

It is possible to prescribe external finishes on the experiment which will maintain temperatures within the specified limits for orbital lifetimes on the order of 2 weeks. However, due to many uncertainties and changes in energy fluxes, a passive system will not successfully operate over 3-month or longer lifetimes.

APPENDIX D

DISTRIBUTION

Code		No. of Copies
AF 5	AFMTC (AFMTC Tech Library-MU-135) Patrick AFB, Fla.	1
AF 18	AUL Maxwell AFB, Ala.	1
AF 32	OAR (BROS, Col. John R. Fowler) Tempo D 4th and Independence Ave, Wash 25, D. C.	1
AF 33	AFOSR, OAR (SRYP) Tempo D 4th and Independence Ave, Wash 25, D. C.	1
AF 43	ASD (ASAPRD – Dist) Wright-Patterson AFB, Ohio	1
AF 124	RADC (RAYLD) Griffiss AFB, New York Attn: Documents Library	1
AF 139	AF Missile Development Center (MDGRT) Holloman AFB, New Mexico	1
AF 314	Hq. OAR (RROSP, Maj. Richard W. Nelson) Washington 25, D. C.	1
AF 318	ARL (ARA-2) Library AFL 2292, Building 450 Wright-Patterson AFB, Ohio	1
Ar 5	Commanding General USASRDL Ft. Monmouth, N.J. Attn: Tech Doc. Ctr. SIGRA/SL-ADT	1
Ar 9	Department of the Army Office of the Chief Signal Officer Washington 25, D. C. Attn: SIGRD-4a-2	1
Ar 50	Commanding Officer Attn: ORDTL-012 Diamond Ordnance Fuze Laboratories Washington 25, D. C.	1

Code	Organization	No. of Copies
Ar 67	Redstone Scientific Information Center U.S. Army Missile Command Redstone Arsenal, Alabama	1
G 31	Office of Scientific Intelligence Central Intelligence Agency 2430 E Street, N.W. Washington 25, D.C.	1
G 2	ASTIA (TIPAA) Arlington Hall Station Arlington 12, Cirginia	20
G 109	Director Langley Research Center National Aeronautics and Space Administration Langley Field, Virginia	1
N 9	Chief, Bureau of Naval Weapons Department of the Navy Washington 25, D. C. Attn: DLI-31	2
N 29	Director (Code 2027) U.S. Naval Research Laboratory Washington 25, D. C.	2
I 292	Director, USAF Project RAND The Rand Corporation 1700 Main Street Santa Monica, California THRU: AF Liaison Office	1
M 6	AFCRL, OAR (CRXRA – Stop 39) L. G. Hanscom Field Bedford, Mass. (mail separately)	20
AF 253	Technical Information Office European Office, Aerospace Research Shell Building, 47 Cantersteen Brussels, Belgium	1
Ar 107	U.S.Army Aviation Human Research Unit U.S. Continental Army Command P.O. Box 428, Fort Rucker, Alabama Attn: Maj. Arne H. Eliasson	1

Code	Organization	No. of Copies
G 8	Library Boulder Laboratories National Bureau of Standards Boulder, Colorado	2
M 63	Institute of the Aerospace Sciences, Inc. 2 East 64th Street New York 21, New York Attn: Librarian	1
M 84	AFCRL, OAR (CRXR, J. R. Marple) L. G. Hanscom Field Bedford, Mass.	1
N 73	Office of Naval Research Brance Office, London Navy 100, Box 39 F. P. O., New York, N. Y.	10
U 32	Massachusetts Institute of Technology Research Laboratory Building 26, Room 327 Cambridge 39, Massachusetts Attn: John H. Hewitt	1
U 431	Alderman Library University of Virginia Charlottesville, Virginia	1
G 9	Defence Research Member Canadian Joint Staff 2450 Massachusetts Avenue, N. W. Washington 8, D. C.	1
AF 353	ESD (ESRDC, Mr. Jonas Hallgrimson) L. G. Hanscom Field Bedford, Mass.	1
	Lockheed Missiles & Space Co. Sunnyvale, California	20
	Hq. AFCRL, OAR (CRRKP, Ming S. Wong) L. G. Hanscom Field, Bedford, Mass.	19
G 68	Scientific and Technical Information Facility Attn: NASA Representative (S-AK/DL) P. O. Box 5700 Bethesda, Maryland	1

Office of Aerospace Research, Electronics Research Directorate, Air Force Cambridge Research Laboratories, L. G. Hanscom Field, Massachusetts.
Rpt No. AFCRL-63-4. SATELLITE-TO-SATELLITE PROPAGATION EXPERIMENT FEASIBILITY STUDY AND PRELIMINARY DESIGN. Scientific rpt no. 1, Dec 62, 67p. incl. illus., 4 refs.

Unclassified Report

The effects of the ionosphere upon radio frequency electromagnetic waves are discussed. Several types of satellite-to-satellite propagation experiments are presented, and the problems of implementation are delineated. The equipment around which the experiment must be designed is described, as are the vehicles available in Program 162. The relative merits of the various vehicles and the basis for the selection of the experimental configuration are discussed. The preliminary design results

(over)

1. Propagation
2. Ionospheric Propagation
I. OAR Project 4603
Task 460307
II. Contract AF19(628)-457
III. Lockheed Missiles & Space Co., Sunnyvale, California
IV. J. Meyer
V. Aval fr OTS
VI. In ASTIA collection

Office of Aerospace Research, Electronics Research Directorate, Air Force Cambridge Research Laboratories, L. G. Hanscom Field, Massachusetts.
Rpt No. AFCRL-63-4. SATELLITE-TO-SATELLITE PROPAGATION EXPERIMENT FEASIBILITY STUDY AND PRELIMINARY DESIGN. Scientific rpt no. 1, Dec 62, 67p. incl. illus., 4 refs.

Unclassified Report

The effects of the ionosphere upon radio frequency electromagnetic waves are discussed. Several types of satellite-to-satellite propagation experiments are presented, and the problems of implementation are delineated. The equipment around which the experiment must be designed is described, as are the vehicles available in Program 162. The relative merits of the various vehicles and the basis for the selection of the experimental configuration are discussed. The preliminary design results

(over)

1. Propagation
2. Ionospheric Propagation
I. OAR Project 4603
Task 460307
II. Contract AF19(628)-457
III. Lockheed Missiles & Space Co., Sunnyvale, California
IV. J Meyer
V. Aval fr OTS
VI. In ASTIA collection

Office of Aerospace Research, Electronics Research Directorate, Air Force Cambridge Research Laboratories, L. G. Hanscom Field, Massachusetts.
Rpt No. AFCRL-63-4. SATELLITE-TO-SATELLITE PROPAGATION EXPERIMENT FEASIBILITY STUDY AND PRELIMINARY DESIGN. Scientific rpt no. 1, Dec 62, 67p. incl. illus., 4 refs.

Unclassified Report

The effects of the ionosphere upon radio frequency electromagnetic waves are discussed. Several types of satellite-to-satellite propagation experiments are presented, and the problems of implementation are delineated. The equipment around which the experiment must be designed is described, as are the vehicles available in Program 162. The relative merits of the various vehicles and the basis for the selection of the experimental configuration are discussed. The preliminary design results

(over)

1. Propagation
2. Ionospheric Propagation
I. OAR Project 4603
Task 460307
II. Contract AF19(628)-457
III. Lockheed Missiles & Space Co., Sunnyvale, California
IV. J. Meyer
V. Aval fr OTS
VI. In ASTIA collection

Office of Aerospace Research, Electronics Research Directorate, Air Force Cambridge Research Laboratories, L. G. Hanscom Field, Massachusetts.
Rpt No. AFCRL-63-4. SATELLITE-TO-SATELLITE PROPAGATION EXPERIMENT FEASIBILITY STUDY AND PRELIMINARY DESIGN. Scientific rpt no. 1, Dec 62, 67p. incl. illus., 4 refs.

Unclassified Report

The effects of the ionosphere upon radio frequency electromagnetic waves are discussed. Several types of satellite-to-satellite propagation experiments are presented, and the problems of implementation are delineated. The equipment around which the experiment must be designed is described, as are the vehicles available in Program 162. The relative merits of the various vehicles and the basis for the selection of the experimental configuration are discussed. The preliminary design results

(over)

1. Propagation
2. Ionospheric Propagation
I. OAR Project 4603
Task 460307
II. Contract AF19(628)-457
III. Lockheed Missiles & Space Co., Sunnyvale, California
IV. J. Meyer
V. Aval fr OTS
VI. In ASTIA collection

are shown. The development of a program to calculate vehicle separation as a function of separation velocity increment and time from separation is presented for the no-drag case.

are shown. The development of a program to calculate vehicle separation as a function of separation velocity increment and time from separation is presented for the no-drag case.

are shown. The development of a program to calculate vehicle separation as a function of separation velocity increment and time from separation is presented for the no-drag case.

are shown. The development of a program to calculate vehicle separation as a function of separation velocity increment and time from separation is presented for the no-drag case.